Performance of metallic auxetic needle drives

F Dalcanale[1], JP Kirchhofer[1], F Schuler[1], L Rubbert[2], P Renaud[2], M de Wild[1]

[1] *University of Applied Sciences Northwestern Switzerland, FHNW, School of Life Sciences, Institute for Medical Engineering and Medical Informatics IM², Muttenz, Switzerland.*
[2] *INSA-ICUBE, Strasbourg, France.*

INTRODUCTION: The aim of this study is the development of a metallic 3D-printed auxetic needle drive for a robot [1] dedicated to interventional radiology and image guided surgery.

METHODS: Auxetic structures were designed with SolidWorks™ (Dassault Systèmes, France) and produced in titanium by selective laser melting (SLM, DMG Mori, Germany) [2]. Quadratic 4-balloon (Fig. 1a) and pentagonal 5-balloon designs (Fig. 1b) with different strut widths and thicknesses were generated, see Fig. 1c and Tab. 1. Due to the auxetic lattice structure of the actuator, axial expansion is achieved at pressure increase of the 4 or 5 inflated catheter balloons located within the unit [3]. The video analysis and modelling tool (*Tracker* software [4]) was used to quantify the performance of the different designs based on 10 s video sequences (3840 x 2160 pixel, 30 fps).

RESULTS: Fig. 2 shows the change in length of different designs with increasing internal pressure. The axial elongation at 4 bar d_{max} is also listed in Tab. 1.

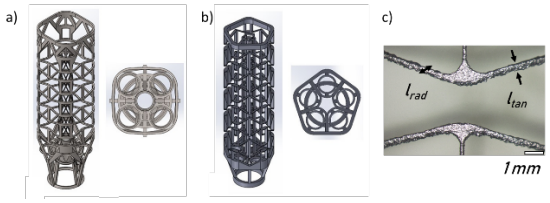

Fig. 1: a) Quadratic and, b) pentagonal auxetic structures with a central guide channel of the biopsy needle. c) Dimensioning of the metallic struts in radial l_{rad} and tangential l_{tan} direction.

Table 1. Design and performance of three versions of quadratic (Q) and pentagonal (P) actuators.

	l_{rad} [mm]	l_{tan} [mm]	*Aspect ratio*	*CS* [mm²]	d_{max} [mm]
Q1	0.54	0.62	0.8:1	0.33	0.16
Q2	0.56	0.40	1.4:1	0.22	0.44
Q3	0.56	0.47	1.2:1	0.26	0.36
P1	1.11	0.28	4.0:1	0.31	1.03
P2	1.14	0.36	3.2:1	0.41	0.57
P3	0.87	0.37	2.4:1	0.32	0.30

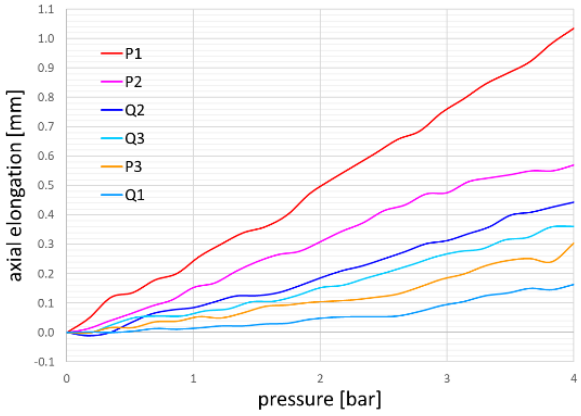

Fig. 2: Axial expansion of pentagonal (P) and quadratic (Q) auxetic titanium actuator variants after increasing the pressure of the inner balloons.

DISCUSSION & CONCLUSIONS: The SLM printing process allows precise production of complex-shaped metallic actuators with different strut geometries in sub-mm precision. The combination of a large ratio of radial to tangential length l_{rad}/l_{tan} with a small cross-sectional area *CS* promotes the movement in the axial direction. This study confirms the pneumatic drive principle of auxetic titanium structures and shows the significant influence of the area moment of inertia of the struts $I_{ax} \cong \frac{l_{rad} l_{tan}^3}{12}$.

REFERENCES: [1] http://spirits.icube.unistra.fr. [2] F. Schuler, P. Renaud, M. de Wild, 3D-printed auxetic structures for bio-medical application, *European Cells and Materials, Online Periodical*, Coll 2, ISSN 1473-2262, 10 (2018). [3] A. Pfeil, L. Barbé, B. Wach, A. Bruyas, F. Geiskopf, M. Nierenberger, et al. A 3D-Printed Needle Driver Based on Auxetic Structure and Inchworm Kinematics. *ASME IDETC 2018;* V05AT07A057. [4] https://physlets.org/tracker/.

ACKNOWLEDGEMENTS: The SPIRITS project is supported by the Region Grand Est, Land Baden-Württemberg, Land Rheinland-Pfalz, Cantons Baselstadt, Basellandschaft, Aargau, Swiss Confederation and by the program INTERREG Upper Rhine from the ERDF (European Regional Development Fund).

In-situ fracture analysis of 3D-printed structures

M Meier[1], F Schuler[1], M de Wild[1]

[1] *University of Applied Sciences Northwestern Switzerland, FHNW, School of Life Sciences, Institute for Medical Engineering and Medical Informatics IM², Muttenz, Switzerland*

INTRODUCTION: Patient-specific titanium implants can be manufactured using additive manufacturing techniques (SLM, Selective Laser Melting). In this study, the mechanical limits of simple and complex-shaped structures were systematically investigated microscopically as well as macroscopically.

METHODS: For strain measurements, micro samples were investigated in-situ in a scanning electron microscope (SEM) while applying increasing mechanical load. The deformation behaviour, the strain fields, the crack propagation and the failure mechanism were evaluated using DIC (Digital Image Correlation) on a sequence of SEM images. The micro specimens were produced from titanium grade 4 by Selective Laser Melting on a SLM-125 system (DMG Mori, Germany) in a vertical orientation. Various specimen geometries with 300 µm nominal thickness were designed: dog bone samples (l_0 = 500 µm, d_0 = 500 µm), diamond (s_0 = 1.4 mm, d_0 = 300 µm), single and double strut structures (l_0 = 3.6 mm, d_0 = 500 µm), see Fig. 1. In-situ tensile tests were performed in a SEM (TM3030Plus, Hitachi, BSE detector) strain-controlled with a speed of 100 µm/min up to failure using a tensile test table (Deben, UK, 300 N load-cell with 1% resolution, linear inductive displacement sensor with a resolution of 3 µm) while imaging the specimen and recording the stress-strain curve. The strain field is obtained and quantified from a series of SEM images at different applied forces by *Ncorr*, an open-source 2D digital image correlation software [1].

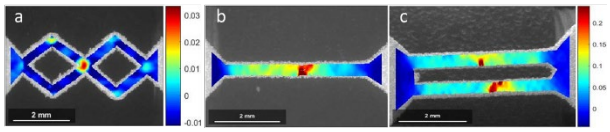

Fig. 1: Optical Eulerian strain fields ε_{xx} by SEM-DIC while tensile testing a) a diamond, b) a single and c) a double strut structure before fracturing. Scale bars indicate 2 mm.

RESULTS: The DIC overlays in Fig. 2a-h show the zoned deformation behaviour and peak stress of a dog bone specimen when loaded up to 105 N. The samples produced show approximately 40% smaller cross-sectional area than originally designed by CAD, see Fig. 3.

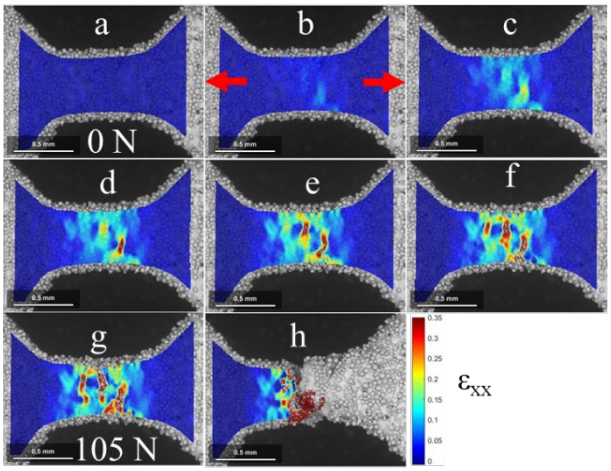

Fig. 2a-h: Plastic deformation bands perpendicular to the tensile loading direction (red arrows in b) are observed in the DIC analysis of an SLM micro specimen mechanically stressed in the SEM even before surface cracks occur. Scale bars indicate 500 µm.

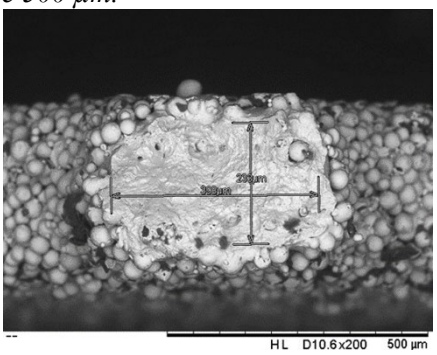

Fig. 3: Geometrically determined area of fracture with Ti particles sintered to the surface.

DISCUSSION & CONCLUSIONS: Zonal deformation ε_{xx} is much higher than the overall strain observed before fracture [2]. The SLM-related decoration-particles can be used as reference points so the SEM-DIC can thus be performed directly on untreated SLM samples. However, these spherical particles may occasionally cause slippage within the fixture.

REFERENCES: [1] www.ncorr.com. [2] P. Schüler, S.F. Fischer, A. Bührig-Polaczek, C. Fleck (2013) *Mat Sci Eng A* **587**:250-261.

A cryogel platform for differentiation and transplantation of dopaminergic neurons in treatment of Parkinson's disease

A Filippova[1], L Efremova[1], KH Krause[1], T Braschler[1]

[1] *Department of Pathology and Immunology, Centre Médicale Universitaire, University of Geneva, Switzerland*

INTRODUCTION: Human pluripotent stem cells (hPSCs) have great potential in cell replacement therapy for Parkinson's disease [1]. At the moment, transplantation of mature hPSC-derived neurons is practically impossible, due to their fragility and intolerance to pre-transplantation dissociation and handling. Most frequently, hPSC-derived neural precursor cells (NPCs) are thus used for transplantation purposes [1, 2]. While NPCs are more tolerant, such transplantation may lead to patient-dependent variability in the outcome and unpleasant side effects, due to lack of control over the final differentiation.
In order to have better control over the final differentiation and avoid excessive handling, we propose using a slowly biodegradable porous carboxymethyl cellulose-based cryogel (CMC) scaffold [2] as a structural support during differentiation and transplantation.

METHODS: CMC cryogels were produced using carbodiimide-based crosslinking [3]. Coating molecules were covalently bound to the cryogels using carbodiimide chemistry and labeled by rhodamine isothiocyanate (RITC).

LUHMES cells or hESC cells were seeded onto the scaffolds and differentiated according to published protocols. Neuronal adhesion and cell phenotype was characterized using immunocytochemistry and confocal microscopy. Gene expression was determined using qPCR. Viability was evaluated using Alamar Blue assay or Calcein/PI staining.

24 GA syringe was used for injection of the 0.4 mm ⌀ scaffolds.

RESULTS: Cryogel coating conditions were adapted for highest protein adhesion on the biomaterial and highest neural spread along the cryogel walls. Dopaminergic neurons were obtained from LUHMES cells and hESC-derived NPCs inside the cryogel scaffold. Passage of neuron-containing scaffolds through a 24 GA syringe resulted in minimal viability loss, compared to near-complete cell loss of neurons differentiated in 2D.

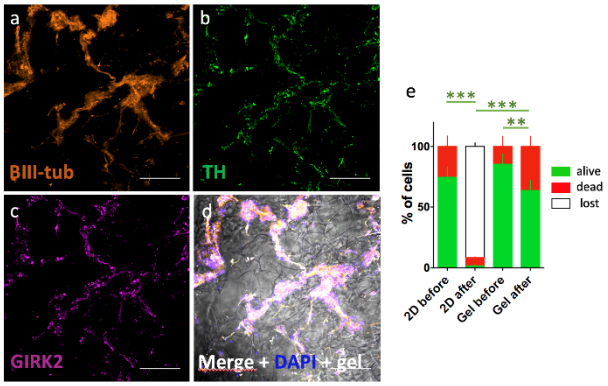

Fig. 1: a-d. hESC-derived neurons, differentiated on the cryogel (day 41). Immunocytochemical staining of neuron (BIII-tub) and dopamine neuron (TH+GIRK2) markers. e. Cell survival after passage of neurons cultured in 2D or neuron-containing cryogel through an injection needle.

DISCUSSION & CONCLUSIONS: Out of three adhesion molecules, laminin 111 showed the best neuronal adhesion. Optimal coating conditions were selected for best neurite spread along the scaffold. Similar NPC differentiation phenotype was obtained in 2D and inside the scaffolds. Passage of neuron-containing scaffolds through an injection needle resulted in substantial preservation of viable cells, compared to 2D cultured neurons.

Using cryogel scaffolds in cell replacement therapy would allow pre-transplantation graft characterization and help preserve neuronal architecture during transplantation procedures. Upon subsequent in vivo injection of the scaffold into the striatum, the porosity of the biomaterial would potentially facilitate perfusion of the scaffolds with innate neurotrophic factors and help graft integration into the endogenous neuronal network.

REFERENCES: [1] CW Olanow et al. (2009) *Neurology* **21** Suppl 4:S1-136. [2] S. Nolbrant et al. (2017) *Nat Prot* **12**:1962–1979. [3] A. Béduer, T. Braschler et al (2015) *Adv Healthc Mater* **4** (2): 301-12.

T-Cadherin (CDH13)-positive cells in the stromal vascular fraction of human adipose tissue are key players for vasculogenesis and osteogenesis

J Guerrero[1,3], B Dasen[1], A Frismantiene[2], S Pigeot[1], TJ Resink[2], I Martin[1], A Scherberich[1]

[1] University of Basel Hospital, Department of Biomedicine, Tissue Engineering, Basel, CH, [2] University of Basel Hospital, Department of Biomedicine, Laboratory of Signal Transduction, Basel, CH, [3] Department for BioMedical Research (DBMR), University of Bern, Bern, CH

INTRODUCTION: The stromal vascular fraction (SVF) of human adipose tissue is a heterogeneous cell population isolated from native adipose by enzymatic digestion of the tissue and centrifugation to remove lipid-laden adipocytes. SVF contains adipose mesenchymal stromal cells (ASC), vascular cells (endothelial cells (ECs) and pericytes), hematopoietic cells (i.e. monocytes and macrophages) and many other cell types. In the field of bone tissue engineering, the joint vasculogenic and osteogenic potential of human SVF cells was demonstrated in numerous in vitro, preclinical and even clinical studies [1]. However, the specific role of ASCs (bone-forming cells) and ECs (vessel-forming cells), and their interaction in supporting bone and blood vessels' formation is only poorly understood. In the present study, we identified T-cadherin (T-Cad), a GPI-anchored member of cadherin superfamily, as a specific marker of EC in SVF and investigated the role of T-Cad-positive ECs in bone and vessel formation by SVF cells in vivo.

METHODS: T-Cad expression was investigated by immunofluorescence in native human adipose tissue and on unpassaged (Unpass) long term expanded ASCs. Cell sorting to remove T-Cad+ cells was performed on SVF and Unpass cells which were then cultured inside a ceramic scaffold (Engipore) with a perfusion bioreactor system for 5 days. We investigated the angiogenic and osteogenic potential of the generated cell-ceramic constructs upon subcutaneous implantation in nude mice for 12 weeks.

RESULTS: T-Cad expression in native human adipose tissue was observed specifically in ECs residing on the laminin-positive basement membrane of adipose vessels (Fig. 1A, B). SVF cells cultured as monolayer showed a gradual decrease of the expression of T-Cad in passaged cells. In a previous study, we showed that even minimal expansion on plastic caused a significant loss of ASCs' osteogenic potential [2]. Here, at passage 4, expression of T-Cad was reduced by more than 75%. In Unpass cells *in vitro*, T-Cad was expressed, but only by CD31-positive ECs present inside self-assembling pseudo-vascular networks (Fig. 1C). SVF cells depleted in T-Cad$^+$ cells-based constructs showed dramatically decreased bone tissue formation capacity and human blood vessels' formation after *in vivo* implantation as compared to un-depleted SVF cells. Unpass cells depleted in T-Cad$^+$ cells showed a very similar trend. The *in vivo* bone formation by T-Cad-depleted cell populations could be fully rescued by addition of human umbilical vein-derived ECs, confirming the key and specific role played by ECs in bone formation by ASCs. The relying mechanisms are currently being investigated, in particular the role of VEGF, adiponectin and IGF-1.

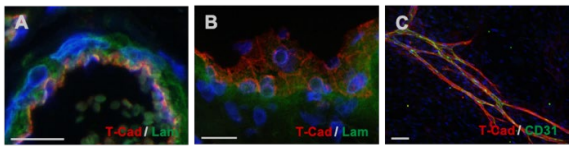

Fig. 1: Characterization of T-Cadherin-positive cells. (A, B) Immunofluorescence on native human adipose tissue for T-Cad and Laminin. (C) Immunofluorescence on Unpass cells for T-Cad and CD31. Abbreviation: T-Cad, T-Cadherin; Lam, Laminin. Scale Bar = 100 µm.

DISCUSSION & CONCLUSIONS: The processes of angiogenesis and osteogenesis are thought to be dependent on a close interaction between bone-forming ASCs and ECs. In this study, we demonstrated that the T-Cad+ ECs present in native human adipose tissue and SVF cells and kept in Unpass cells play a critical, indispensable role in the bone forming capacity of human adipose-derived cells. The involved mechanisms need to be further investigated. The present findings should allow for a better control of the osteogenic potential of adipose-derived cells, to maximize the performance of engineered grafts in the context of clinical bone regeneration.*location.*

REFERENCES: [1] F. Saxer, A. Scherberich, A. Todorov, et al (2016) *Stem Cells* **Dec;34(12)**:2956-2966. [2] A. Scherberich, R. Galli, C. Jaquiery, J. Farhadi, I. Martin (2007) *Stem Cells* **Jul;25(7)**:1823-9.

ACKNOWLEDGEMENTS: This study was supported by the Swiss National Science Foundation, SNF Grant 310030-138519.

Alginate-based microreactors as support for osteoblasts to enhance biomineralization

F Itel[1,2], J Skovhus[3], B Städler[2]

[1]Laboratory for Biomimetic Membranes and Textiles, Empa, Swiss Federal Laboratories for Materials Science and Technology, 9014 St. Gallen, Switzerland. [2]Interdisciplinary Nanoscience Center, University of Aarhus, Aarhus, Denmark. [3]Department of Biomedicine, University of Aarhus, Aarhus, Denmark

INTRODUCTION: Inspired by nature, cell mimicry is an emerging field that aims to provide long-lasting cell-like assemblies to stimulate their biological counterparts with broad envisioned applications in biomedicine. [1] Encapsulation of nanometer-sized functional entities within micro-meter-sized carriers are the common concepts to design functional microreactors. However, their influence on biological cells remains little explored, especially when considering aspects beyond cell viability.

Here, we assembled alginate-based microreacters that resemble the basic function of bone cells. With the microreactor's ability to initiate mineralization and, thus, stimulate neighboring osteoblast cells, our goal is to kick-start biomineralization. [2] As the bioactive moiety, we selected osteoblast-derived matrix vesicles (MVs), which are encapsulated within the hydrogel matrix (Fig 1. left). MVs are ~100 nm-sized lipid vesicles that are secreted by osteoblasts and are the initial mechanism of bone mineralization. In order to force the cells to interact with the microreactors, we chose a spheroid model as study system, where cell-to-cell and cell-to-particle interactions are promoted (Fig. 1, middle). The effect of the bone cell mimics on bone-forming osteoblast cells (SaOS-2 cells) was investigated by quantifying the produced mineral of the spheroids.

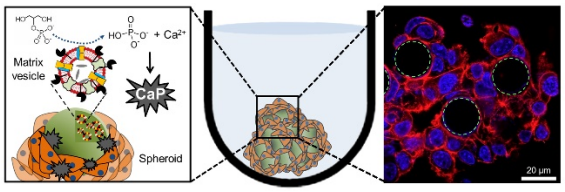

Fig. 1: Schematic overview of the cell-microreactor spheroid with microreactor function, and fluorescent microscopy cross-section image of cells co-assembled with alginate microparticles.

METHODS: The 50 µm-sized alginate particles are generated using droplet-microfluidics. The MV-equipped microreactors are assembled by mixing MVs with alginate. Cell attachment on the alginate particle surface was achieved by poly-L-lysine coating. Cell viability within the spheroids was assessed by live-dead staining. Mineralization was quantified by micro-computed tomography (µCT) and by determining the calcium content per spheroid. Cells-only spheroids and empty microreactors served as controls.

RESULTS: SaOS-2 cells co-assembled with alginate microparticles as stable spheroids (Fig. 1 right). Cell viability within the spheroids was significantly increased most probably due to the enhanced nutrient availability in presence of the microparticles compared to cells-only spheroids. In presence of MV-microreactors, the mineral amount on day 3 was already significantly increased compared to controls, as validated by the calcium quantification and µCT analysis, and on day 14, there was 50% more calcium present than the cells-only control. This strongly indicates the beneficial impact of the MVs within the alginate microparticles on the biomineralization.

DISCUSSION & CONCLUSIONS: Here, we equipped alginate microparticles with SaOS-2-derived MVs to generate bone cell mimics with the ability to stimulate biological SaOS-2 cells when cocultured as spheroids and kick-start biomineralization. The results indicate that combining the fields of cell mimicry and bone tissue engineering may lead to improved osteoconductive and osteoinductive scaffolds by the integration of micro-reactors. Furthermore, the microreactors can not only stimulate cells but also can maybe reduce the number of cells needed in a scaffold by the replacement with their artificial counterparts. We anticipate that our artificial cells can be used in different forms and shapes, not only as spheres, but also as surface coating.

REFERENCES: [1] F. Itel, P. Schattling, Y. Zhang, B. Städler (2017) *Adv. Drug Deliv. Rev.* **118**, 94-108. [2] F. Itel, J. Skovhus Thomsen, B. Städler (2018) *ACS Appl. Mater. Interfaces* **10**, 30180-30190.

ACKNOWLEDGEMENTS: This work was supported by grants from the Aarhus University Research Foundation, Denmark and the Swiss National Science Foundation.

Embroidered Medical Textiles - Numerous possibilities for the creation of tailor-made mesh implants by technical embroidery

C Elschner[1], L Bittrich[1], A Breier[1], J Hahn[1], A Spickenheuer[1]

[1]*Leibniz-Institut für Polymerforschung Dresden e. V. (IPF), Dresden, Germany*

INTRODUCTION: Embroidery technology is the textile manufacturing process that offers the greatest flexibility for designing textile structures and is traditionally associated with decorative textile finishing. However, the classic embroidery process can also be used for the manufacturing of medical products. For about 15 years, research projects have been carried out at the IPF with the aim of producing biocompatible porous structures out of surgical suture materials. Mesh implants with flexible network design are produced by the specific selection of embroidery parameters such as stitch length and stitch angle [1, 2]. As a proof of concept, a digital Embroidery Pattern Generator (EPG) was to be designed to create stress-adapted and tailor-made hernia meshes.

METHODS: A standard industrial embroidery machine was used (ZSK JCZ 0209-550). The embroidery patterns are created software-based using a program with Python programming language, which makes all parameters accessible via a graphical user interface and calculates a corresponding mesh. The output is in the EDOpath format (Complex Fiber Structures GmbH, Dresden, Germany).

RESULTS: Fig. 1 illustrates two different designs for basic structures, exemplarily. The maximum pore diameter of base mesh 1 is 2.8 mm, the maximum diameter of the second pattern is considerably larger and is 4.2 mm, theoretically.

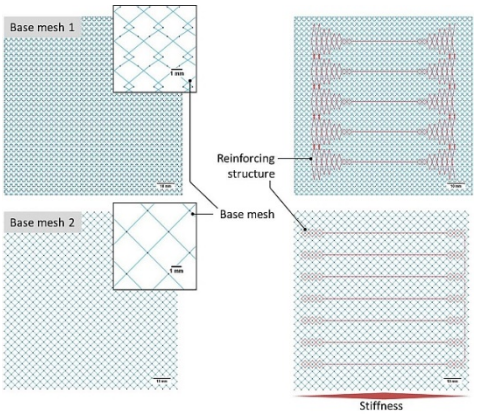

Fig. 1: Computer-aided generation of embroidery patterns for possible mesh implants. Left row: two different basic patterns; right row: basic pattern with reinforcement structure.

The pore sizes of embroidered meshes are smaller than the theoretically calculated sizes and depend on the thread thickness of the surgical suture material used.

DISCUSSION & CONCLUSIONS: With the help of the EPG various mesh patterns and mesh sizes can be generated very easily. Homogeneous basic structures can be reinforced with specific patterns to obtain anisotropic meshes. The mechanical properties are determined by the material selection and essentially by the design. Embroidered anisotropic mesh implants could be advantageous for hernia surgery because they can locally strengthen the hernia of the abdominal wall or groin, but do not unnecessarily stiffen the healthy tissue in the marginal area due to greater elasticity. Regarding to the great heterogeneity of the patients, there can be no one-fits-all solution [3]. Embroidery technology opens up the possibility of patient-specific hernia meshs.

REFERENCES: [1] A. Breier, L. Bittrich, J. Hahn, A. Spickenheuer (2017) *Evaluation of optical data gained by ARAMIS-measurement of abdominal wall movements for an anisotropic pattern design of stress-adapted hernia meshes produced by embroidery technology*, IOP Conf. Ser.: Mater. Sci. Eng. **254 6:** 062002. [2] Hahn J, Bittrich L, Breier A, Spickenheuer A (2017) *Stress adapted embroidered meshes with a graded pattern design for abdominal wall hernia repair*, IOP Conf. Ser.: Mater. Sci. Eng. **254 6:** 062005. [3] Klinge U, Klosterhalfen B (2018) *Mesh implants for hernia repair: an update,* Expert Rev Med Devices **15 10:** 735-746.

ACKNOWLEDGEMENTS: This work was carried out during the IGF project 18790 BR. The authors thank the Federal Ministry of Economic Affairs and energy (BMWi) for financial support. In addition, the authors would like to thank the project partners involved: Institute of Textile Machinery and High Performance Material Technology (ITM) at TU Dresden and Centre for Translational Bone, Joint, and Soft Tissue Research (TFO) at the University Hospital Dresden.

Flexible lactide copolymer as hydrogel reinforcement

E Tosoratti[1], P Fisch[1], MS Taylor[2], M Zenobi-Wong[1]

[1]Tissue Engineering + Biofabrication, ETH, Zürich, CH. [2]Poly-Med, Inc, Anderson SC, USA

INTRODUCTION: Hydrogels can provide a biocompatible environment for cells, but their overall mechanical properties are too weak and brittle to maintain their shape for long periods of time *in vivo* [1]. A novel flexible lactide copolymer is used as a reinforcement material to provide soft tissue implants with additional mechanical stability.

METHODS: A lactide copolymer (Poly-Med, Inc, Anderson SC, USA) is 3D printed using a 10% wiggle pattern in the shape of 6 mm cylinders and used as a reinforcement material. Human auricular chondrocytes (10 million/ml) are encapsulated in 1.5% hyaluronic acid transglutaminase crosslinked gel (HATG), a hydrogel previously developed in our laboratory[2], and embedded in the reinforcement material. The biocompatibility of the reinforcement material alone and of the reinforced HATG construct is assessed by means of live/dead staining, compression testing, histology and *in vivo* subcutaneous implantation. In the *in vivo* study, HATG + reinforcement precultured samples are compared to non-precultured samples. Samples are explanted at day 63.

RESULTS: Live/dead staining at days 1-21 of culture showed over 95% cell viability in the HATG + reinforcement samples. Collagen matrix deposition was observed at day 21 (Fig. 1).

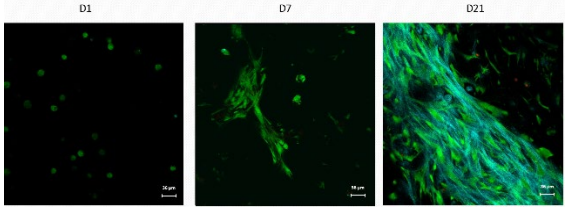

Fig 1: Live/Dead staining of in vitro cell culture of HATG + lactide reinforcement

The compressive modulus of 1.5% acellular HATG was of 6 kPa. As shown in Figure 2, the chondrocytes embedded in HATG + reinforcement showed a steady increase in stiffness between day 1 (33 kPa) and day 21 (257 kPa). Between day 21 and day 63 no additional increase in stiffness was measured. *In vivo* precultured samples showed a higher stiffness compared to non-precultured samples (Fig. 2) at explantation.

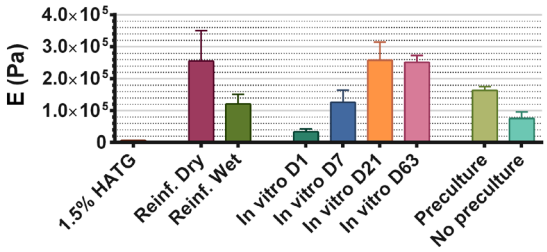

Fig 2: Compressive modulus (E) of the various samples under 15% strain compression

Histology (Fig. 3) of both *in vitro* and *in vivo* samples showed good collagen and GAG deposition, both indicative of a chondrogenic tissue.

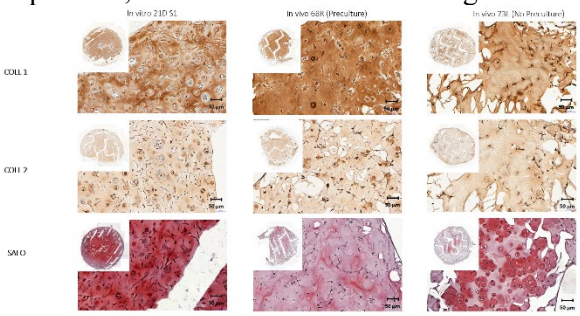

Fig 3: Collagen I and II and GAG production in both in vitro (day 21) and in vivo (day 63) samples

CONCLUSION: The compressive modulus of 1.5% HATG hydrogel increased six-fold thanks to the addition of the lactide reinforcement. The reinforced construct continued to develop *in vitro,* reaching 257 kPa compressive modulus in 21 days. The steady-state of the stiffness from day 21-63, instead of the expected continued increase in stiffness, may involve the simultaneous degradation of the polymer reinforcement expected during this time period. The tunability of mechanical properties and degradation rate of the 3D printed constructs offer a unique system to balance matrix deposition and biopolymer degradation to achieve implants with uniform mechanical properties over time.

REFERENCES: [1]J. An, et al (2016) *Mineralization processes in hard tissue*, Bone, Biomineralization and Biomaterials. [2]Nicolas Broguiere, et al (2016), *Factor XIII Cross-Linked Hyaluronan Hydrogels for Cartilage Tissue Engineering*, ACS Biomaterials Science & Engineering.

Novel biomimetic approach for titanium surface treatment by calcium phosphate: towards the production of implants with improved bioactivity

A Carino[1], A Testino[1], E Mueller[2], M de Wild[3], F Dalcanale[3], P Gruner[4], W Moser[5], B Hoechst[6]

[1] Paul Scherrer Institut, ENE-LBK, Villigen, CH, [2] Paul Scherrer Institut, BIO-EMF, Villigen, CH, [3] School of Life Sciences FHNW, Institute for Medical Engineering and Medical Informatics, Muttenz, CH, [4] Medicoat AG, Maegenwill, CH, [5] Atesos Medical AG, Aarau, CH. [6] Hager & Meisinger GmbH, Neuss, DE

INTRODUCTION: The interface between implant and bone is one of the critical factors to achieve short healing time and long term stability. We applied a wet, biomimetic, cost-effective route to activate the surface of titanium implants with a thin calcium phosphate phase. A ceramic micro- and nanostructured surface, strongly joined to the metal, is obtained.

METHODS: The method developed was applied to titanium grade 4 discs with different micro-topography such as polished, sandblasted, sandblasted and acid etched, similarly to what is commercially available [1]. The calcium phosphate (CaP) treatment is done under a novel controlled biomimetic approach [2, 3], promoting the heterogeneous nucleation and growth of the ceramic phase on the metal. The treatment is done by in-situ and on-line monitoring of the deposition. As a consequence, the control over thickness, chemical phases and morphology of the ceramic layer is obtained (Fig. 1). The CaP treatment is carried out after an alkaline-thermal step (a modified version of the Kokubo method [4]). The Ti surface is transformed into a highly porous layer of hydrogen sodium titanate ceramics of few microns (grafting layer, GL), which is chemically bonded to the metal.

RESULTS: A thin layer of CaP nucleates and growths under biomimetic condition within the GL. The nanostructured deposited material has a solubility higher than that of mature hydroxyapatite and, should be resorbed and promote the formation of natural bone in-vivo. Moreover, the experimental conditions for CaP formation can be tuned to stimulate the formation of octacalcium phosphate (OCP), which is considered the precursor of natural bone. Both GL and CaP modifications generate a nanostructured morphology, which also enhances wettability. Concurrently, the microroughness induced by blasting or etching is preserved. The synergistic effect of micro- and nanostructure is expected to shorten healing time and promote osseointegration [5].

DISCUSSION & CONCLUSIONS: A thin synthetic bone layer is deposited in a controlled manner on Ti substrate being firmly grafted to it. The GL ensures that CaP does not delaminate after mechanical stress. The modified surface is expected to improve the implant bioactivity.

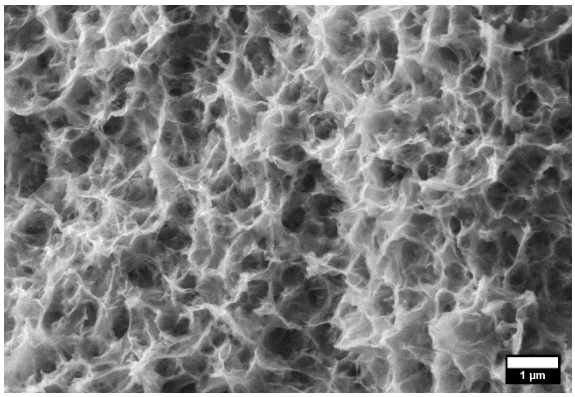

Fig. 1: Micrograph of the nanostructured Ti surface after modification with CaP.

REFERENCES: [1] Nicolau, P., *et al.* (2018). *10-year outcomes with immediate and early loaded implants with a chemically modified SLA surface.* Quintessence Int: **2**-12. [2] PCT/EP2018/076267. [3] T. Kokubo, *et al*. (2010) *Bioactive Ti Metal and its Alloys Prepared by Chemical Treatments: State-of-the-Art and Future Trends*, Advanced Biomaterials **12**:B597. [4] A. Carino, *et al.* (2018) *Formation and transformation of calcium phosphate phases under biologically relevant conditions: Experiments and modelling*, Acta Biomaterialia **74**: 478. [5] Gittens, R. A., et al. (2014). *Implant osseointegration and the role of microroughness and nanostructures: Lessons for spine implants* Acta Biomaterialia **10**: 3363.

ACKNOWLEDGEMENTS: We thank the Swiss Nanoscience Institute and Medicoat AG for the financial support, and Hager & Meisinger for supplying the implants.

.

Biological response of Polycarbonate-Urethane articulation on cartilage – a pin-on-disc in vitro study

LT Dal Fabbro[1], R Lerf[2], B Schmid[1], D Baumgartner[1], L Vainieri[3]

[1] *Zurich University of Applied Sciences, Institute of Mechanical Systems (IMES)*
[2] *Mathys AG, Bettlach, CH.* [3]*AO Research Institute, AO Foundation, Davos, CH*

INTRODUCTION: Approximately 5% of the human population and 80 % of people above 65 years suffer from shoulder osteoarthritis (OA) [1]. Nowadays total shoulder replacements are performed to treat severe cases of OA. In 30 – 40% of the cases, even a healthy glenoid is replaced rather than using a hemiprosthesis because they are known for wearing off cartilage relatively fast [2]. In previous studies polycarbonate-urethane (PCU) showed a 3 fold smaller coefficient of friction against cartilage compared to traditional orthopaedic materials indicating that PCU might be a promising coating for hemiprostheses [3]. The aim of this thesis is to develop a pin-on-disc tester and to test the usability of PCU as a coating for hemiprostheses.

METHODS: A pin-on-disc tester was developed, which allows the testing with different materials, variable loads, variable sliding velocities, and different two-dimensional testing paths. Cartilage pins were extracted from both condyles of bovine knees and tested against 3 different biomaterials: zirconia toughed alumina (ZTA), cobalt chrome alloy (CoCr) and PCU. Tests were conducted with above-physiological loads (test 1) to see differences in wear and surface structure, as well as with physiological loads (test 2) to see the reaction of the living tissue (only ZTA and PCU were tested). The surface morphology of the articular cartilage was then analysed and the loss of cartilage height measured (test 1). A Safranin-o (SAF-O) and lactate dihydrogenase (LDH) staining were performed to show the viability of the chondrocytes post-test (test 2).

RESULTS: Microscopic images showed striking differences in cartilage surface morphology after testing (test 1) against the different biomaterials (Fig. 1). The ZTA group showed a significantly greater decrease in height compared to the PCU group (Fig. 2). There was no significant difference in decreased height between the samples tested with CoCr and PCU. The SAF-O staining showed increased fibrillation on the articulating surface in both tested groups compared to the control group. The LDH staining showed a very high viability in all samples.

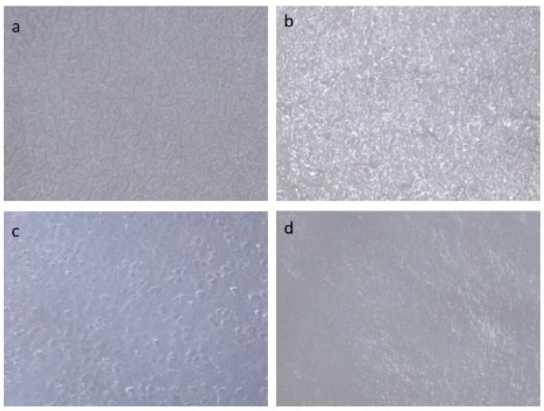

Fig. 1: Surface morphology after testing (test 1) a) PCU, b) ZTA, c) CoCr and d) control group.

DISCUSSION & CONCLUSIONS: Although articulation of PCU and CoCr showed around three fold lower cartilage height loss than ZTA, the histological assessment did not find significant differences between treatments. Thus it remains uncertain whether PCU would be a better choice for hemiprostheses coating than CoCr and ZTA. To validate the results, further tests (test 2) with longer test time and greater sample number need to be performed.

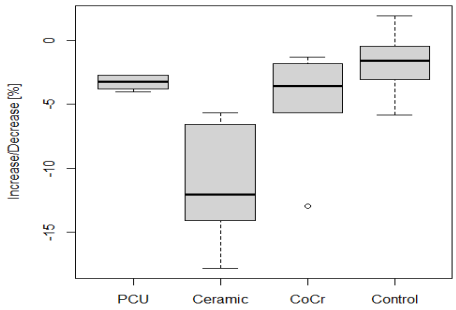

Fig. 2: Boxplot of decrease in cartilage height after testing (test1) (n=6 for each group).

REFERENCES: [1]L. Shi, et al (2011) *Annals of Biomedical Engineering*, pp 132-146. [2] J. Lizhang, et al. (2013) *Journal of engineering in medicine* **227**(12) 1284-1291 [3]J. Sague, et al. (2013) *CORS Venice*.

Self-assembling peptide hydrogels and their versatile beneficial properties for the treatment of periodontal disease

F Koch[1], S Saxer[1], U Pieles[1], K Peters[2], B Kreikemeyer[2]

[1] Institute of Chemistry and Bioanalytics, University of Applied Sciences Northwestern Switzerland, Muttenz, CH, [2] Institute of Medical Microbiology, Virology and Hygiene, University Medicine Rostock, Rostock, DE

INTRODUCTION: Periodontitis is an oral inflammatory disease affecting 50-60% of the adult world population [1]. Periodontitis is mainly caused by the invasion of pathogenic bacteria which leads to the destruction of the alveolar bone and the periodontal ligament. The application of self-assembling peptides (SAP) is of great interest for periodontal therapy, as they are injectable and can be modulated to fulfill hard and soft tissue requirements. Moreover, based on their hydrogel surface properties and their swelling ability, they can act as a bacteria membrane disruptor as well as a drug carrier. To verify this hypothesis, we tested four peptide sequences, (designed by Aggeli *et al* [2]) and demonstrated their usefulness as excellent scaffold based on their tunable stiffness, favorable degradation rates, soft and hard tissue regeneration potential, antimicrobial activity and their drug delivery capability.

METHODS: SAP hydrogels (15 mg/ml) were prepared in Tris- NaCl buffer (0.055 M Tris; 0.192 M NaCl, pH 7.0). Hydrogel stiffness was measured by oscillatory rheology. Human primary periodontal ligament fibroblasts (HPLF) and human calvarial osteoblasts (HCO) were used as a model for periodontal tissue structures. Tissue regenerative potential was determined by measuring cytotoxicity (using LDH kit), cell growth (by PrestoBlue®Viability Reagent) and osteogenic differentiation (Bioplex Kit). Antimicrobial activity was assessed by monitoring the optical density (600 nm) of *P.gingivalis* after 48 h incubation on SAP hydrogels. Moreover a live/dead fluorescent staining was performed. SAP hydrogels were loaded either with ciprofloxacin, tetracycline or doxycycline at 150 mg/L. The release were measured using HPLC-MS.

RESULTS: By varying the peptide concentration and buffer composition, a wide range (0.6-205 kPa) of hydrogel stiffnesses has been achieved [3]. A maximum SAP hydrogel degradation of 20 % was observed for different buffer solutions after 7 days. The stability regarding enzymatic and bacterial digestion showed less degradation in comparison to the degradation rate in buffer. Cytocompatibility (HCO, HPDLF) studies revealed no cytotoxic effect for P11-SAP hydrogels. Metabolic activity after 24 h varied from 40 to 80 % depending on the SAP properties. Significantly enhanced osteogenic degree was detected for SAP hydrogels compared to cells cultured on control surfaces [4].

Antimicrobial activity was mainly found for highly charged positive SAP hydrogels against *P.gingivalis* (see Fig.1B). The bactericidal effect could be even enhanced by adapting the SAP concentration (Fig.1C) [5].

The incorporation of antibiotics did not affect fibril formation and resulted in favourable release kinetics up to 120 h [5].

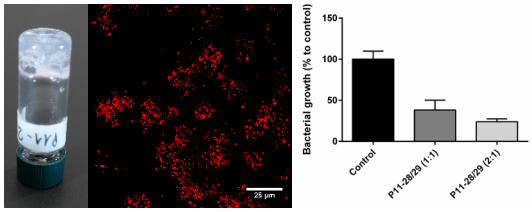

Fig. 1: Antimicrobial activity of positively charged P11-28/29 hydrogel (left) on P.gingivalis. After 48 h incubation time, dead bacteria were visualized with propidium iodide (middle) and bacterial growth were monitored at an optical density of 600 nm (right).

DISCUSSION & CONCLUSIONS: In summary, P11-SAP hydrogels combine many favourable& tuneable properties required to make them applicable as a prospective novel treatment strategy for periodontal therapy.

REFERENCES: [1] J. Shaju (2012), *International Arab Journal of Dentistry*, v3, n.1[2] A. Aggeli et al (2001) Self-assembling peptide systems in biology, medicine, and engineering, *Springer*. [3] F. Koch et al (2018), *R. Soc. Open Sci*., 5, 171562. [4] F. Koch et al (2018), *Int. J. Nanomed.*, *13*, 6717-33. [5] F. Koch et al (2019), accepted in *Adv. Healthcare Mater.*

ACKNOWLEDGEMENTS: We thank Michael Hug and Dominik Lysek (credentis AG) for funding and supporting this work and for the valuable discussions.

.

Peptide nanorod structures made by pH-induced self assembly process

SS Saxer[1], L Kind[1]

[1] *University of Applied Sciences & Arts FHNW, Muttenz, Switzerland*

INTRODUCTION: Short self-assembling peptides such a the 11-mers (P11-4) are used as biocompatible hydrogels. During β-sheet assembly, they first form well defined fibres and then build a three dimensional, random mesh structure comparable to collagen [1]. They are of prominent interest as the self-assembly process occurs under physiological conditions, it can be locally induced by simple salt or pH changes and is reversible [2]. This is an advantageous feature for nondestructive access of cavities such as for example the remineralization of dental lesions [3].

We intend to use the benefits of the first, defined fibre formation step but prevent the formation of the random mesh structure by introducing polymer-peptide-conjugates that sterically interrupt the beta sheet formation and thus lead to short peptide fibrils, a type of organic, biocompatible peptide nanorods (PNRs). Similar to prevailing nanocellulose, such PNRs are applicable as nanocarriers, filler, vaccines etc. for application in drug delivery, tissue engineering, medtech, woundhealing and biologics. Other than nanocellulose, the formation of the defined PNR's is obtained by a reversible self-assembly process and offers additional features such as triggered release and degeneration in cavities etc.

METHODS: Peptide gels were formed from P11-4 undecamer with the sequence Ac-QQRFEWEFEQQ-NH_2 and ATTO647-P11-4 (Ac-QQRFEWEFEQQSGSGC- (ATTO647)-NH_2) at different ratio of Atto-modified and unmodified P11-4 peptides (1:2, 1:5, 1:20 and pure P11-4 as reference). Peptide were dissolved in TRIS (20mM, pH=8.4) and assembled under addition of 0.5µL phosphoric acid (0.88% pH=3.5) per 5µL peptide solution and incubation for 12 hours at 4°C. Transmission electron microscopy (TEM) measurements were performed on a Zeiss EM900 by drying the peptide on Formvar/Carbon coated Copper grid (200mesh, ElectronMicroscopy Sciences Ltd.) and uranylacetate staining (2µL of a 2% solution for 2 min per grid).

RESULTS: In the context of toot lesion therapy, fluorescent peptides were used to proof the diffusion and assembly in the lesions. The implementation of the fluorescent Atto-647 Marker (MW: 642.908 g/mol) into the peptide sequence was expected to seriously influence the assembly process. Therefore mixtures with different ratio of Atto-modified and unmodified P11-4 peptides were assembled. The fibre structures of the dried hydrogel were measured with transmission electron microscopy (TEM, Fig. 1). The images clearly show a fibre formation but with increasing ratio of Atto-P11-4 the fibers were of shorter length, which gives a hint of disturbed fibre structure (beta fold structure) and thus led to the idea of a closer investigation of such PNRs.

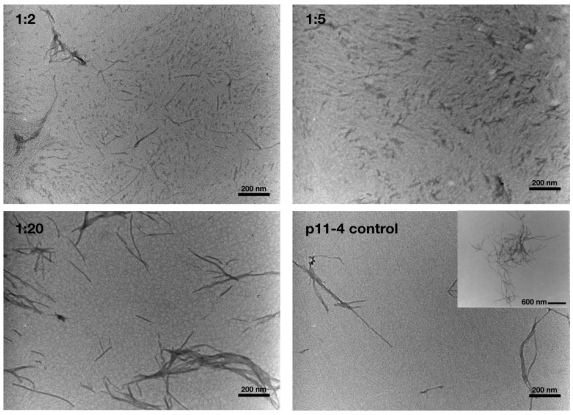

Fig. 1: Effect of the sterically larger Atto-P11-4 on fibre structure, with descending ratio of Atto P11-4 to unmodified P11-4 (top left). TEM pictures taken at 50 kx magnification with a Zeiss EM900. Samples were stained with uranylacetate.

DISCUSSION & CONCLUSIONS: TEM images show a clear evidence that an increased amount of large side groups linked to the N-terminus of P11-4 peptides interrupt the formation of fibrous 3d mesh structure. These preliminary findings require to be further investigated in terms of side group type and size, concentration and resulting fibre length. Moreover we intend to use this effect to guide fibre formation and to form well-defined, reversible PNRs or even more complex structures.

REFERENCES: [1]R.P. Davies, A. Aggeli, N. Boden, McLeish TC, Nyrkova IA, Semenov AN. (2009) *Adv. chem. engin. 35: 11-43.* [2]F. Koch, M. Müller, F. König, N. Meyer, J. Gattlen, U. Pieles, K. Peters, B. Kreikemeyer, S. Mathes, S. Saxer (2018), *R. Soc. open sci.*5:171562. [3]L. Kind, S. Stevanovic, S. Wuttig, S. Wimberger, J. Hofer, B. Müller, and U. Pieles, (2017) *J. Dental Res.*96: 790-797. 0

ACKNOWLEDGEMENTS: The authors contributed equally to the project and would kindly thank credentis AG for their support.

Co-culturing of neural cell lines enables survival in serum-free conditions: towards 3D culture of mixed neural cell types

B Schwendele[1], R Guzman[1, 2], M Gullo[3], D Trueb[3], P Kunz[3], M Schmid[3], J Koeser[3]

[1] University Hospital Basel, Department of Biomedicine, Basel, CH, [2] University Hospital and Children's Hospital of Basel, Department of Neurosurgery, Division of Pediatric Neurosurgery, Basel, CH, [3] School of Life Sciences, FHNW, Muttenz, CH

INTRODUCTION: To study possible paracrine signalling of different cell types, we embedded cells in a suitable hydrogel, in which cell-cell contacts are mainly avoided and where the individual cell types can be arranged in specific patterns in space. To evaluate the suitability of the hydrogel, the results were compared to those of a classical 2D approach.

METHODS: BV2 microglia and C17 neural stem cells (NSC) were cultured in DMEM + 10% FCS and seeded as single cell cultures or co-cultures in 24 well plates either directly (2D) or embedded in 4% gelatin (3D). The next day the medium was exchanged for serum free DMEM and the cells were cultured further for up to 16 days. For the quantification of surviving cells in 2D and 3D culture the resazurin reduction assay was applied, cell proliferation was determined by BrdU or EdU incorporation. Cell morphology was controlled by brightfield microscopy and images were focus stacked with fiji-imageJ.

RESULTS: When BV2 and C17 cells were grown in DMEM under serum free conditions proliferation gradually decreased and only few cells survived after 16 days (Fig 1a, b). In contrast, when both cell types were co-cultured the metabolic signal of the culture gradually increased indicating survival of the cells. The rescuing effect was larger when the co-culture was set up with more C17 than BV2 cells (9:1 ratio). While this effect was observed both in 2D and 3D culture most of the time no clearly segregated colonies of the two cell types were observed in 2D culture which might be due to detaching and reattaching as well as migrating cells. In contrast, under 3D conditions segregated BV2 and C17 colonies were observed (Fig 1c). C17 cells under such co-culture conditions developed long extensions at prolonged culture time (30d, Fig. 1d). In a further development both cell types were bioprinted in segregated areas in a newly developed methylcellulose-gelatin bioink and, as observed before, cell survival was largely improved when both cell types were co-printed in the same culture dish indicating a paracrine mechanism of action.

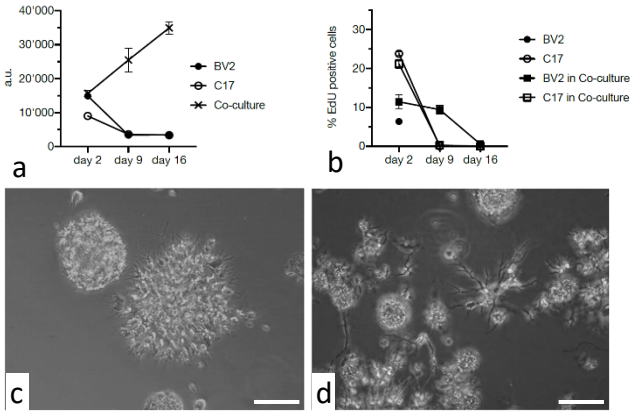

Fig. 1: Survival and proliferation of BV2 and C17 cells in single vs. co-culture under serum free conditions. Development of the metabolic activity (a) and proliferation rate (b) of cultures during 16 days. c) BV2 (up left) and C17 (center) colony morphology in co-culture after 16 days d) morphology of BV2 + C17 co-cultures embedded in gelatin after 30 days. Scalebar 100 µm.

DISCUSSION & CONCLUSIONS: Here we present data demonstrating the beneficial effect of co-cultivating NSC and microglia cell lines on cell survival under serum free conditions. This effect was observed in both 2D and 3D cell culture, while the development of long thin protrusions on C17 cells was more prominent in 3D culture. Next we plan to vary 3D culture conditions with respect to hydrogel stiffness which is known to influence cell differentiation and to investigate the development of defined spatial arrangements of bioprinted multi cell type tissues.

ACKNOWLEDGEMENTS: Funding by an internal grant from the FHNW is gratefully acknowledged.

Fiber geometry in 3D printed scaffolds modulates dynamic cell seeding

L Mainardi[1,2], C Arrigoni[1], E Bianchi[2], G Talò[1,3], M Piergiovanni[2], G Dubini[2], C Candrian[1], M Moretti[1,3]

[1] Regenerative Medicine Technologies Laboratory, Ente Ospedaliero Cantonale, Lugano, CH, [2] Laboratory of Biological Structure Mechanics, Politecnico di Milano, Milano, IT. [3] Cell and Tissue Engineering Laboratory, IRCCS Istituto Ortopedico Galeazzi, Milano, IT

INTRODUCTION: 3D-printing is an additive manufacturing technique, which is increasingly applied to produce fibrous scaffolds in tissue engineering approaches [1]. Although 3D printing allows to precisely control the porous geometry and internal architecture of built objects, standard scaffolds, printed with circular section fibers (CFs), show inadequate numbers of adherent cells after dynamic seeding [2]. The goal of this work was to increase adherent cell number modifying the cross-sectional area of the scaffold fibers.

METHODS: Multi-lobed fibers (MLFs) scaffolds were designed and fabricated through an FDM-based 3D printer, fusing and depositing parallel cylindrical fibers to form composite structures characterized by a non-circular cross-sectional geometry. An oscillating perfusion bioreactor was used to perform dynamic seeding of MG63 cells on PLA cylindrical scaffolds (d=8mm, h=4mm). Cell viability (CV), seeding efficiency (SE) and cell proliferation (CP) were evaluated through Alamar Blue and CyQuant assays after 1, 3 and 7 days of culture. Distribution of adherent cells was analyzed through MTT assays and immunostaining with DAPI and phallacidin after dynamic seeding. Fluid dynamic characterization was performed through computational simulations (CFD) using ANSYS Fluent in volumetric sections of the scaffolds imposing translational periodicity on inlet and outlet, symmetry on lateral sections and no-slip conditions on the fibers. Microfluidic models were developed to study the effect on SE of fluid dynamic modifications induced by the differences in fiber cross-sectional geometry.

RESULTS: A significant increment (p=0.0002*) of SE was observed after dynamic seeding between CFs controls and MLFs scaffolds, demonstrating that fiber cross-sectional geometry can influence the cellular ability to adhere to the scaffolds. MTT assays and immunostaining showed that fiber shape impacts also on cells distribution and morphology, inducing adherent cells to spread and align along the direction of MLFs. CFD simulations allowed to verify that shear stress values induced on CFs and MLFs by a dynamic culturing system remained below the maximum physiological levels. CP and CV of CFs and MLFs scaffolds following 3 and 7 days of culture did not show any significant statistical difference, confirming that MLFs scaffolds are not detrimental for adherent cells and their growth, as compared to controls. Microfluidic models experimentally confirmed that the increment of SE could be associated to the modification of cell trajectories induced by MLFs.

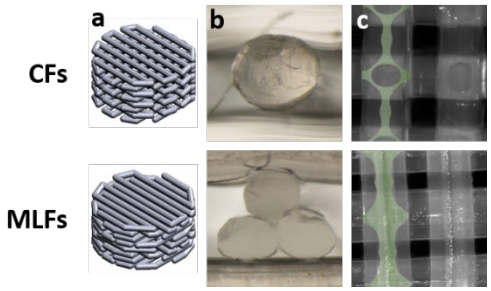

Fig. 1: Designed (a) and printed (b) CFs and MLFs scaffolds. (c) Overlap of simulated low WSS zones (green areas) and detected cell position (white spots).

*Table 1. CV and SE values of CFs and MLFs scaffolds (mean±SD,*p=0.0002)*

	CV [U.I.·10^3]	SE [%]
CFs	50.3±15.2	5.2±3.8*
MLFs	108.1±36.2	18.7±7.8*

DISCUSSION & CONCLUSIONS: Modifying the cross-sectional geometry of deposited fibers in 3D printed scaffolds represents a valid method to improve dynamic SE, enhancing the ability of cells to adhere to them and influencing cell distribution and morphology, without compromising cell growth after 7 days of culture.

REFERENCES: [1] Chen Y et al., *Tissue Eng Part C Methods*. 2011 Dec; 17(12):1211-21. doi:10.1089/ten.tec.2011.0092. [2] Yang S et al., *Tissue Eng.* 2002 Feb; 8(1):1-11. doi:10.1089/107632702753503009.

Use of infant chondrocytes for cartilage repair

A Bonato[1], G Barreto[2], A Gerstenberg[3], D Weber[3], M Zenobi-Wong[1]

[1] Tissue Engineering + Biofabrication, ETH Zürich, CH, [2] Helsinki Rheumatic Diseases & Inflammation Research Group, University of Helsinki, Finland, [3] Division of Hand Surgery, University Children's Hospital Zürich, Switzerland

INTRODUCTION: It is known that hyaline articular cartilage has limited ability to regenerate when injured, and these cartilage lesions can lead to degenerative diseases such as osteoarthritis. Tissue engineering approaches to treat cartilage defects require a high number of cells. Unfortunately, chondrocytes tend to assume a fibroblastic-like appearance and lose the ability to differentiate into cartilage after a few passages, a process called dedifferentiation. This remains one of the main problems for cartilage cell-based therapies.

The aim of this study was to find a way to improve the proliferative and chondrogenic properties of cells used in cartilage repair. Cartilage from polydactyly patients are a source of young and highly proliferative cells that have a higher potential to differentiate compared to adult chondrocytes [1], and were thus used as a source of cells for this project. First, we investigated the chondrogenic properties of a novel stem-like chondroprogenitor population isolated from cartilage of polydactyly patients. Secondly, since proliferation in a 2D environment induces dedifferentiation, we evaluated expansion in a thermoreversible 3D system could enhance the chondrogenic potential of the cells.

METHODS: Chondroprogenitors were isolated through the fibronectin adhesion assay. Briefly, freshly isolated cells were seeded in fibronectin-coated plates for 20 minutes at 37°C, and non-adherent cells were removed and medium changed. After one week, colonies with more than 32 cells were picked with cloning rings, to get rid of terminally differentiated cells. Clones were individually cultured in DMEM, 10% FBS and 5 ng/ml FGF2 until passage 5, then they were pelleted and differentiated in medium containing DMEM, 10% FBS, 10 ng/ml TGFβ3, 50 ug/ml ascorbic acid, 40 ug/ml L-proline and 1% ITS+ for three weeks.

To test effects of a 3D environment during expansion and if this could prevent cell dedifferentiation after extensive passaging, freshly isolated chondrocytes were grown in 3D culture in thermoreversible MeBiol® hydrogel (Cosmo Bio) with DMEM, 10% FBS and the addition of 5ng/ml FGF2, 1ng/ml TGFb1, or 100 ng/ml IGF-1.

RESULTS: Chondroprogenitors proliferated to reach a Population Doubling Level (PDL) of 46 at passage 4 and of 53 at passage 5. They also retained the ability to produce GAGs and collagens (Fig.1).

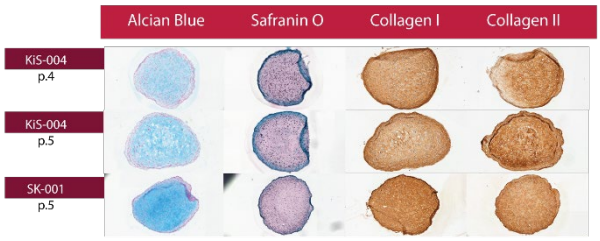

Fig. 1: Chondrogenesis pellet assay. Pellets were cryosectioned and stained for Alcian blue, Safranin O (GAGs), Collagen I and Collagen II.

Cells grown in the thermoreversible hydrogel showed high viability (> 94%). All three growth factors enhanced proliferation, with the best result in the IGF-1 condition. (Fig.2).

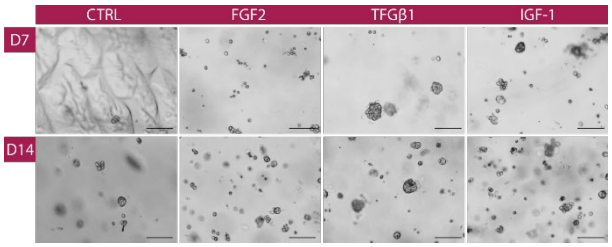

Fig. 2: Brightfield of chondrocytes in Mebiol® Gel after 7 and 14 days in culture with normal expansion medium and with addition of FGF2, TGFβ1 or IGF-1. Scale bar 100µm.

DISCUSSION & CONCLUSIONS: Infant chondroprogenitors show a high proliferative potential, along with the ability to redifferentiate at high PDLs. The thermosensitive 3D culture has the potential to allow cell expansion in 3D without concomitant de-differentiation.

REFERENCES: [1]E. Cavalli et al, (2019) *Sci Rep,* **9**: 4275.

Development of a perfusion bioreactor-based in vitro model to evaluate the osteoinductive capacity of granular bone substitutes

T Klein[1], J Bürgin[1], K Shankar[2], W Hoffmann[2], I Martin[1], A Scherberich[1]

[1] Department of Biomedical Engineering, University and University Hospital of Basel, Basel, CH, [2] Nobel Biocare Services AG P.O. Box, CH-8058 Zürich-Flughafen, Switzerland

INTRODUCTION: We recently developed *in vitro* bone models to investigate the effect of drugs on bone metabolism [1]. The aim of the present study was to develop a 3D perfusion bioreactor-based *in vitro* model, to evaluate the capacity of granular bone substitutes to support osteoblastic differentiation of osteoprogenitors.

METHODS: 3D cultures were established with a perfusion bioreactor system (CELLEC Biotek AG). Two 100 µm pore grids, combined to custom-fabricated medical-grade poly-ether-ether-ketone (PEEK) ring adaptors, were used to confine the granules inside the perfusion bioreactor system (Fig. 1). $3x10^6$ cells from an immortalized stromal cell line (M-SOD) or primary human bone marrow-derived mesenchymal stromal cells (hBM-MSCs) were perfused overnight through 200 mm^3 of 2 novel bovine xenografts (HA & HA+) granules (0.25-1 mm) at a superficial velocity of 1 mm/s. Bio-Oss (Geistlich Pharma) granules with similar granulometry were used as control. After 24 h (cell seeding phase), cells were cultured at a reduced superficial velocity of 100 µm/s for 3 weeks with an osteoinductive medium. Cells were retrieved by perfusing a solution of collagenase at 1 mm/s for 40 minutes, followed by 10 additional minutes with a solution of 0.05% trypsin/0.53 mM EDTA. Extracted cells were counted in a Neubauer chamber. The number of un-extracted cells –i.e. remaining inside the granules- was evaluated by DNA quantification (Cyquant). After harvesting, cells were incubated for 30 minutes at 4°C with antibodies directed against human CD29, CD90 and CD146. Cells were then analysed by cytofluorimetry. Cells were also used for analysis of osteoblastic gene expression by real-time PCR for the following genes: Runx2, collagen type I, alkaline phosphatase and osteopontin.

RESULTS: The initial cell seeding efficiency was deduced by analysing the number of non-adhered cells in the supernatant at first medium change and was ≥ 80 % for all materials. The use of M-SOD cells resulted in a much higher cellularity (5-10 million cells per construct) than when hBM-MSCs were used (0.5-1.5 million cells per construct). However, M-SOD cells were not only present inside the granules but also on the grids and in the chamber space. By contrast, hBM-MSCs remained exclusively confined inside the granules. HA xenograft material supported a significantly higher cellular content with hBM-MSCs (2.3-fold compared to HA+, 1.8-fold to Bio-Oss, $p<0.0001$). There was no relevant difference in mesenchymal protein expression (CD29, CD90 and CD146). HA+ material induced a significantly higher expression of the osteoblastic genes runx2 and osteopontin as compared to the 2 other tested materials.

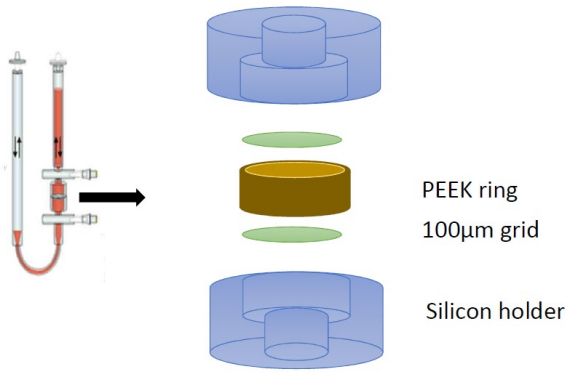

Fig. 1: Perfusion bioreactor setting for the test of granulate materials.

DISCUSSION & CONCLUSIONS: We successfully developed and validated a perfusion-based model of osteoblastic differentiation for the testing of granule materials. Both M-SOD and hBM-MSCs identified a superiority of HA+ bovine xenograft over other test materials in the induction of osteoblastic differentiation. The model should be further validated, by introducing negative and positive control materials. A refinement of the readouts, e.g. additional osteoblastic gene in PCR or quantification of calcium release, is also envisioned.

REFERENCES: [1] E. Rossi E, A.Scherberich, *Tissue Eng Part C Methods.* 2018; **24**(7):391-398.

PDMS based multi electrode arrays for electrical and optical cortex recordings in vivo

AF Renz[1], C Lewis[2], J Lee[1], K Tybrandt[3], F Helmchen[2], J Vörös[1]

[1] *Laboratory of Biosensors and Bioelectronics ETH Zürich, Switzerland.*
[2] *Laboratory of Neural Circuit Dynamics, University of Zurich, Switzerland.*
[3] *Science and Technology, University of Linköping, Sweden*

INTRODUCTION: New approaches for the fabrication of stretchable electronic implants in healthcare applications have attracted increased attention in the past years. Enhancement of the implant-tissue interface to both reduce the foreign body response as well as achieve improved electrode properties has been the main focus of many new devices.[1] Stretchable implants have shown promise in their ability to reduce the foreign body response, however, there are still many limitations to the successful implementation of these devices. Especially, achieving the combination of reliable electrical, as well as optical recordings could open new possibilities in neuronal research.

METHODS: By incorporating synthesized gold nanowires [2] as a track layer and platinum particles as electrodes in PDMS, a fully conductive and stretchable electronic implant was generated. Over a straight forward filtration process on a pre-patterned PVDF membrane [3], a defined conductive pattern was gained. These were then transferred onto pre-cured PDMS and insulated with a PDMS top layer. After electrochemical characterization the full devices were mounted on the cortex of transgenic GCaMP6 mice. Several experiments in anesthetized animals were conducted to test the potential of this multimodal platform as a tool for neuroscience.

RESULTS: Here, we present the combination of the two approaches by using PDMS based electronic implants to gain scattering free optical recordings through this transparent base material. The highly porous platinum electrodes allow for specific temporal resolution and the processed PDMS shows sufficient visibility to record the spatial resolution by 2-photon imaging. We were able to generate multimodal neuronal recordings in living animals in first proof-of-concept experiments.

DISCUSSION & CONCLUSIONS: By fabricating PDMS based electronic implants with a newly generated protocol, new designs, sizes and unconventional shapes can be incorporated within a short time frame. This approach shows promising results for the versatile use of PDMS based implants for complex brain activity recordings.

REFERENCES: [1]Renz et al(2018) A guide towards long-term functional electrodes interfacing neuronal tissue. *J. Neural Eng*. **15** 061001. [2]Tybrandt et al(2018) High-Density Stretchable Electrode Grids for Chronic Neural Recording. *Adv. Mater.* **15** 1706520. [3]Flurin Stauffer et al(2016) Bright Stretchable Alternating Current Electroluminescent Displays Based on High Permittivity Composites. *Adv. Mater.* **33** 7200-7203.

ACKNOWLEDGEMENTS: We would like to thank Steven Wheeler, Aldo Rossi and ScopeM for visualizing our technical ideas and their support, ETH Zurich and the SNF for the funding.

Surface modification of drug delivery microspheres to enhance affinity to bone

SG Rotman[1], DW Grijpma[2], RG Richards[1], TF Moriarty[1], D Eglin[1], O Guillaume[1]

[1] AO Research Institute Davos, Davos, CH. [2] Department of Biomaterials Science and Technology, Faculty of Science and Technology, Technical Medical Centre, University of Twente, Enschede, The Netherlands

INTRODUCTION: The efficacy of antibiotic treatments for bone infections is limited due to insufficient availability of antibiotics coupled with a low penetration of antibiotics in bone tissue [1]. Local antibiotic-loaded biomaterials are often bulky and release antibiotics with sub-optimal diffusion-based kinetics. In this work, we present a biodegradable poly(ϵ-caprolactone) (PCL) microparticulate system, for antibiotic delivery. The particle surface is functionalized with chelators to establish particle affinity to bone mineral. A comparison in terms of hydroxyapatite (HAP) complexation is made between alendronate (ALN) and oligomers of aspartic acid (ASP) as chelators present on the particle surface.

METHODS: PCL microparticles were fabricated by oil/water emulsion with 10% PCL (MW = 80,000 g·mol^{-1}) and 2.5% Gentamicin-AOT in dichloromethane as an organic phase and 1% poly(vinyl alcohol) as an aqueous phase. Antibiotic encapsulation and subsequent release was measured by fluorometric assays. Antimicrobial properties of the particles were observed for 5 days. As a next step, the PCL microparticles were exposed to 0.1M NaOH in order to enrich the surface with carboxylic acid moieties. EDC/NHS conjugation was applied to covalently bind ALN or ASP to the carboxylated surface of the particles. Affinity of the functionalized particles to HAP substrates (films and scaffolds) was tested by exposing the substrate to 1 mg/mL particle dispersion. Quantification of chelated particles to HAP substrates was made by measuring fluorescence from pyrene encapsulated in the bound particles.

RESULTS: PCL microparticles with a size average of 0.80 ± 0.47 µm (Fig. 1A) and a Gentamicin-AOT load of 10.0% w/w were fabricated. The microparticles showed a sustained release of antibiotic over a 2-week period, releasing 60% of their load in this period. The MIC of the particles against *S. aureus* was determined to be 9.76 µg/mL and the inhibitory zone of 1 mg of microparticles was observable for 5 days. The formation of carboxylic acid groups on the surface of the PCL microparticles was confirmed with Fourier-transform infrared spectroscopy (FTIR). After EDC/NHS conjugation of ALN, an increase in complexation with a HAP films could be measured (Fig. 1B). PCL-ALN particles were observed on the HAP scaffold by scanning electron microscopy (SEM). Conjugation with ASP in similar manner resulted in slightly lower binding to a HAP film compared to PCL-ALN.

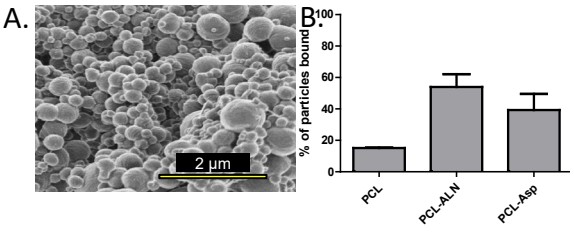

Fig. 1: A. PCL microspheres with a gentamicin-AOT load of 10 wt%. B. Increased affinity to HAP after particle surface functionalization with chelators ALN and ASP (n=3)

DISCUSSION & CONCLUSIONS: ALN functionalized PCL microparticles had higher affinity to HAP substrates than PCL-ASP particles. However, as ALN acts an osteoclast inhibitor, the use of ASP might be more favourable when delivering antibiotics to an infected bone fracture where bone remodelling is essential. While the inhibitory properties against *S. aureus* was shown for the antibiotic loaded microparticles, its enhanced affinity to HAP through surface modification provides a way to ensure high doses of antibiotics at the immediate periphery of the bone. By presenting this bone targeting drug delivery system, first steps were made to provide a potential tool for orthopedic surgeons to treat infections of the bone.

REFERENCES: [1] P. Carek et al. (2001) *Am Fam Physician* 63(12):2413-2421

ACKNOWLEDGEMENTS: This work was supported by the AOTrauma Clinical Priority Program Bone Infection.

Ex vivo repair of the degenerated bovine intervertebral disc using an injectable bioadhesive containing adipose-derived mesenchymal stem cells

TR Christiani [1], AJ Vernengo [1]

[1] *Rowan University, Glassboro, NJ 08028, USA*

INTRODUCTION: Discectomy is a prevalent surgical treatment to remove impinging portions of central nucleus pulposus (NP) and/or peripheral annulus fibrosus (AF) from the intervertebral disc (IVD) to alleviate symptoms of lower back pain. This surgery is associated with inferior outcomes and does not restore healthy mechanical function to the joint. Replacing degenerated or ruptured disc tissue using an injectable replacement containing adipose-derived mesenchymal stem cells (AD-MSCs) may have important clinical impact. The proposed injectable replacement is a bioadhesive composite consisting of the thermosesnsitive hydrogel poly (N-isopropylacrylamide-graft-chondroitin sulfate) (PNIPAAm-g-CS) blended with calcium crosslinked alginate microparticles [1].

METHODS: IVD segments were dissected from the caudal region of bovine tails. Discs were cultured in high glucose medium supplemented with 10 % fetal bovine serum, 100 U/mL penicillin, 100 µg/mL streptomycin, 0.25 µg/mL amphotericin B, and 50 µg/mL ascorbic acid while under a free-swelling environment (5% CO_2 and 37 °C). Artificial disc degeneration was initiated using approximately 100 – 200 µL of 100 U/mL papain enzyme and progressed for 7 days. AD-MSCs were cultured in advance, labelled with red fluorescent marker PKH26, suspended in the composite at a density of 5 x 10^6 cells/mL, and injected into degenerated discs. Treated discs (n=3) were cultured for an additional 14 days and compared to intact (n=3) or injured discs (n=3). Viability of native disc cells and AD-MSCs, region-specific morphology and protein deposition by AD-MSCs were assessed at the end of the culture period.

RESULTS: Viability of native NP and AF cells of intact discs was sustained over the course of 14 days under free-swelling culturing conditions. Intact discs showed no changes in biochemical composition or morphological structure. Injection of the papain enzyme degraded NP tissue, thus leaving behind a central void. Enzyme injection caused a minor decline in native disc cell viability near the periphery of the void or in outer regions of the AF. After 14 days of culture, encapsulated AD-MSCs were 86.8 ± 4.9% viable. AD-MSCs exhibited a rounded or elongated morphology at the center or periphery of the composite, respectively (Fig. 1). AD-MSCs had a positive effect on native disc cell survival and prevented further cell death. Staining for aggrecan, type I collagen, and type II collagen proteins (Fig. 2) were evident in specific-regions of the composite.

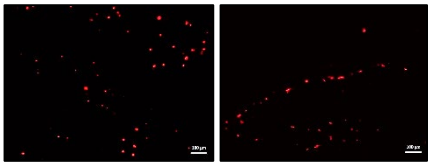

Fig. 1: Fluorescent images of rounded (left) and elongated (right) AD-MSCs at the center and along the periphery of the composite, resp..

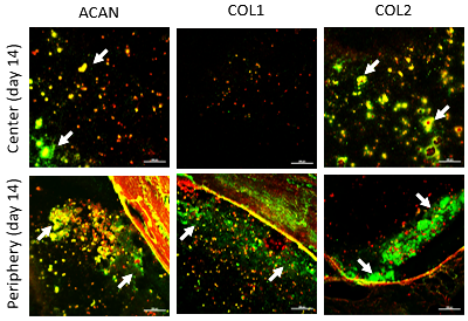

Fig. 2: Immunohistochemical images of aggrecan, type I collagen, and type II collagen staining near AD-MSCs at the center and periphery of the composite.

DISCUSSION & CONCLUSIONS: AD-MSCs undergo chondrogenic differentiation based on the surrounding disc microenvironment. Region-specific differences in cell morphology and protein deposition were identified. Varying grades of disc degeneration, types of annular defects, and mechanical loading will most likely influence site-specific differentiation and should be assessed in future work.

REFERENCES: [1] T.R. Christiani, et al (2016). *J Vis Exp* **116**.

ACKNOWLEDGEMENTS: This research was supported by the New Jersey Health Foundation under Award Nr. PC-2316. The content is solely the responsibility of the authors and does not necessarily represent the official views of the New Jersey Health Foundation.

Hyaluronic acid collagen biomaterial ink with anisotropic properties to control cellular organization

A Schwab[1], L Ambrosio[1], M Alini[1], D Eglin[1], M D'Este[1]

[1] *AO Research Institute Davos, AO Foundation, Davos, CH*

INTRODUCTION: 3D (bio-) printing is an additive manufacturing method to fabricate structured, multi-layered hybrid scaffolds that mimic zonal orientation of extracellular matrix. Here, tyramine modified hyaluronic acid (THA) was combined with collagen I (Col I) to investigate cell instructive properties for application in 3D printing of anisotropic cartilage scaffolds.

METHODS: THA (2.5% w/v) hydrogels were prepared via enzymatic cross-linking using horseradish peroxidase (0.3 – 1.0 U/ml) and hydrogen peroxide [1]. Composite hydrogels were prepared by mixing THA with acidic dissolved Col I (0.5% w/v), isolated from rat tail (THA-Col), and printed with a 3D Discovery (RegenHU). The preservation of fibrillogenesis in the composite hydrogels was evaluated by turbidity measurement (313 nm) over 60 min at 37°C. Col I fibers were visualized by polarized light microscopy and Col I immunostaining of cryo-sections. Cell attachment and cellular alignment on THA and THA-col was evaluated after seeding with bone marrow derived hMSCs by live-dead staining and actin staining of cytoskeleton over time.

RESULTS: Turbidity measurement showed increase in absorbance, indicative of preservation of Col I fibrillogenesis in the composites (Fig. 1A). Col fibers within the double network hydrogels were directly visualized by polarized light microscopy (Fig. 1C) and their presence confirmed by immunostaining for Col I (Fib 1B). THA-Col hydrogels induced hMSC attachment and spreading. For cell encapsulation similar trend was observed: cells were spindle shaped and attached to THA-Col within 1 day whereas MSCs stayed round and did not attach in THA gel, as expected.

DISCUSSION & CONCLUSIONS: Hyaline cartilage is macroscopically homogeneous, but microscopically heterogeneous with zone-dependent orientation of the Col fibers. In this work, we demonstrated the possibility of combining Col and hyaluronan with preservation of Col I fibrillogenesis, resulting in homogeneous constructs with controlled Col I fiber orientation. The constructs showed cell instructive properties by means of modulating cell adhesion and spreading. Presently, we are evaluating how the anisotropic properties of this biomaterial ink influence cell alignment, migration and differentiation. The possibility of printing matrix components with control over macromolecular alignment expands the range of architectures achievable with 3D bioprinting.

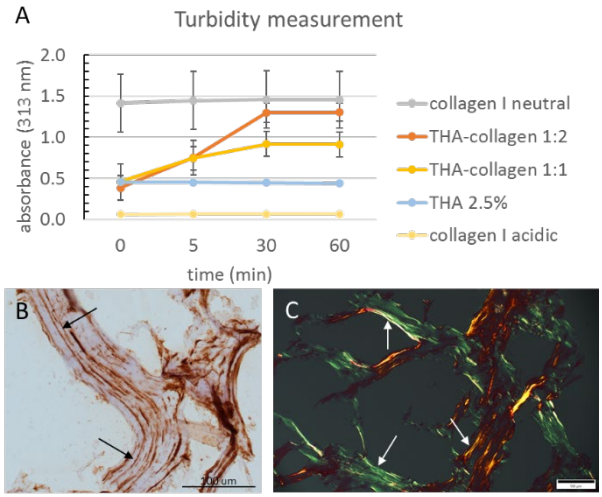

Figure 1. Col I fibrillogenesis and structural organization within THA Col hydrogel: A) Turbidity measurement of Col in presence of THA resulted in an increase in absorbance over time dependent on Col content (n ≥ 3). B) Immunostaining for Col I (scale 100 um) and C) polarized light image (scale 50 um) of THA-col demonstrate fibrillar structure (depicted with arrows).

REFERENCES: [1] Loebel C et al. (2015) *Precise tailoring of tyramine-based hyaluronan hydrogel properties using DMTMM conjugation*, Carbohydr Polym 115: 325-33

ACKNOWLEDGEMENTS: This work is part of the osteochondral defect collaborative research program supported by the AO foundation. The Graubünden Innovationsstiftung is acknowledged for its financial support.

Effects of cell density and doubling number in engineered auricular cartilage

A Martyts[1], P Fisch[1], S Finkielsztein[2], M Zenobi-Wong[1]

[1] Tissue Engineering & Biofabrication Laboratory, Institute for Biomechanics, ETH Zurich, Switzerland. [2] Marine Polymer Technologies Inc

INTRODUCTION: Current state-of-the-art reconstruction surgery for the treatment of microtia is highly invasive as it uses cartilage from the child's ribs to reconstruct the ear and results in modest aesthetic outcomes. Tissue engineering tackles some of these problems and therefore offers an attractive alternative. Using a biopsy as the cell source, patient-specific auricular chondrocytes can be expanded and embedded in a scaffold to fabricate a custom ear. However, a biopsy does not contain enough cells to immediately create an engineered ear, so the chondrocytes must first be expanded for 2-3 passages. In the process, chondrocytes de-differentiate and lose their chondrogenic potential, making them less effective for tissue engineering applications. [1] One way to prevent this is to use low-passage cells as well as fewer cells to create custom ears. In an ongoing experiment, we investigate the effects of cell density and passage number on the in vitro development of engineered auricular cartilage in a hyaluronan transglutaminase (HATG)-based bioink. [2]

METHODS: Primary human auricular chondrocytes were expanded for 2 or 3 passages and embedded in a HATG-based bioink at densities of 1, 5, and 10 million cells/mL. Samples were casted into circular PDMS moulds (1mm high), cross-linked, and cultured in chondrogenic media for 63 days. Cell viability and compressive modulus were assessed at Day 1, 7, 21. Samples were stained using calcein AM and propidium iodide and imaged using a 2-photon microscope (Lecia SP8 MP), with simultaneous collection of the collagen-emitted second harmonic generation signal. Compression tests were performed to 15% strain to measure mechanical development of the constructs (TA.Xtplus, Stable Micro Systems). Experiments were performed with cells from 2 donors.

RESULTS: Samples with $10x10^6$ cells/mL showed highest cell viability (85±6% at Day 7) and proliferation, secreted detectable collagen, and stiffened the most during in vitro culture (Figure 1). Samples containing $5x10^6$ and $1x10^6$ cells/mL showed inferior mechanical properties. The $1x10^6$ cells/mL group had the lowest collagen signal, proliferation, and viability (55±19% at Day 7).

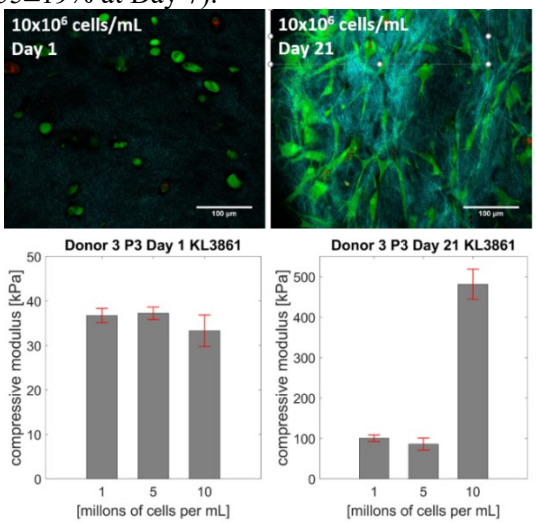

Fig. 1: Top: Live/dead staining at day 1 and 21 of culture. (Calcein AM – green, propidium iodide – red, collagen – cyan). Scale bar 100µm. Bottom: Compressive moduli of constructs at Day 1 and 21. Representative data from one donor shown.

DISCUSSION & CONCLUSIONS: Constructs with $10x10^6$ cells/mL had the highest viability and compressive modulus while $5x10^6$ and $1x10^6$ cells/mL showed lower collagen secretion, viability, and mechanical properties. P2 and P3 constructs developed comparably over 21 days of in vitro culture, but histological analysis of P2 and P3 samples (pending) may reveal differences in cell proliferation, as well as collagen I, collagen II, and glycosaminoglycan deposition. Thus, $10x10^6$ cells/mL is the best tested density for auricular cartilage engineering, but the effects of passage number will be studied further. The experiment is currently being repeated with a third cell donor. To improve the development of lower cell density constructs, addition of adhesion peptides such as RGD and HAV will be investigated next.

REFERENCES: [1] S.W. Kwang, S.P. Yoo, and B.S. Kim (2007) *Biomed Mater Eng*. **17**(5):269-76; [2] N. Broguiere, E. Cavalli et al. (2016) *ACS Biomater. Sci. Eng.* **2** (12):2176–2184.

Establishment of a screening platform for the testing of pro- and anti-angiogenic compounds

LA Krattiger[1], U Blache[1], B Simona[2], MW Tibbitt[3], M Ehrbar[1]
[1] *Laboratory for Cell and Tissue Engineering, Department of Obstetrics, University and University Hospital Zurich, Switzerland.* [2] *Ectica Technologies AG, Zurich, Switzerland.* [3] *Macromolecular Engineering Laboratory, Department of Mechanical and Process Engineering, ETH Zurich, Switzerland*

INTRODUCTION: In recent years, the use of animal models for research has been increasingly frowned upon for several reasons. Tissue-engineered models able to support high-throughput analyses are particularly interesting in pharmaceutical research. The aim of this project is to develop a platform that can be used for basic research, but also in a more clinical context. The platform should enable the study of cellular interactions in angiogenic and vasculogenic events and should furthermore be employable for the screening of pro- and anti-angiogenic factors. It will consist of co-cultures of human endothelial cells and stromal supporting cells embedded into a biomimetic poly(ethylene glycol) hydrogel matrix where they arrange into three-dimensional vessel-like structures within a well-plate format [1,2].

METHODS: Human umbilical vein endothelial cells (HUVECs) and human bone marrow-derived mesenchymal stem cells (BM-MSCs) are encapsulated in fully defined PEG hydrogels. They are cultured at various concentrations of fibroblast growth factor (FGF)-2 for one week. The formation of vascular structures is evaluated by confocal light scanning microscopy for different culture compositions and conditions, such that an overview of tuneable factors influencing the culture outcome is generated. Next, co-cultures will be grown on plates provided by our collaborator, Ectica Technologies AG. These plates contain hydrogels made from the same material as used above for direct encapsulation, however, they are not directly embedded with cells and feature a stiffness gradient. This gradient allows for 3D-ingrowth of vascular co-cultures and is therefore a simple, higher throughput-compatible method for generating 3D vascular structures. Based on previous observations, these cultures will be optimized to be i) reproducible, and ii) sensitive to chemical interventions. Optimized culture systems will then be validated using a library of known pro- and anti-angiogenic factors/compounds. Finally, a screening of new potential drug candidates will be conducted.

RESULTS: We have determined that medium composition, in addition to cell number and co-culture composition have notable effects on the formed network. Cultures grown in the hydrogels predictably feature more vessel-like structures with higher growth factor stimulation. Moreover, increasing the cell number appears to result in increased vessel growth. The ratio of HUVECs to BM-MSCs can be varied, favouring either cell type, while more balanced cultures yield better vascular network formation.

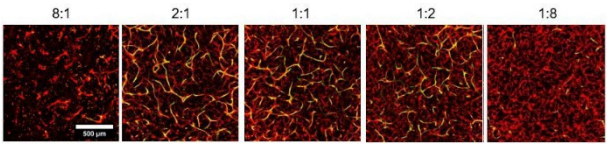

Fig. 1: Maximum projections of confocal stacks of 50 µm. Red: f-actin; green: fluorescent signal from GFP-expressing HUVECs. Ratio of 8:1 denotes eight times more HUVECs compared to BM-MSCs, while the opposite is the case at 1:8.

DISCUSSION & CONCLUSIONS: We have acquired many insights into the possibilities to tune the vasculogenic cultures and similar cultures can also be grown on pre-gelled stiffness gradient hydrogels. However, optimization and validation of these cultures for screening applications is yet to be done.

REFERENCES: [1] U. Blache (2016) *Dual Role of Mesenchymal Stem Cells Allows for Microvascularized Bone Tissue-Like Environments in PEG Hydrogels*, Adv Healthc Mater. [2] N. Zhang et al. (2017) *Soft Hydrogels Featuring In-Depth Surface Density Gradients for the Simple Establishment of 3D Tissue Models for Screening Applications,* SLAS Discov.

Imaging-guided Laser Based Tissue and Biomaterial Preparation for Histology and Biochemical Analysis

H Richter[1], I Bleeker[1], F Will, B Stolze[1]

[1] *LLS ROWIAK LaserLabSolutions GmbH, Garbsener Landstr. 10, 30419 Hannover, Germany*

INTRODUCTION: Preclinical studies in the field of regenerative medicine become more and more important to compete in the market. Histological analysis often is a mandatory, yet laborious part of preclinical study design. Especially the preparation of hard tissue samples or samples containing implants is challenging. Ground section technologies are restricted in section thickness and suffer from high material loss. Alternatively, decalcification of hard tissue for microtomy has to be applied, resulting in loss of biological information. Beyond histology, it becomes more important not only to analyze morphology, but rather to match it with biochemical analysis. Femtosecond laser based cutting of tissue provides novel options of preparing histology sections and 3D-site specific tissue sectioning of further biochemical analysis in one tool.

METHODS: For laser microtomy different types of tissue were plastic embedded, hard tissue without prior decalcification. Sections were prepared by laser cutting at ~10 µm thickness. Histological, immune- and histochemical stainings were applied as indicated in the results. For site-specific 3D-sectioning of native tissue for further molecular analysis, samples from bone-titanium interfaces of a fresh rat tibia were cut at volumes of ~300x300x300 µm. Regions of interest were determined by Optical Coherence Tomography (OCT). Harvested samples were subjected to RNA-extraction and TNF-alpha gene expression analysis.

RESULTS: The results of the histology and histochemistry of tissue sections prepared show that established routine stainings can be successfully applied to thin sections performed by laser microtomy as shown by Hematoxilin and Eosin, Leval Laczko, McNeal or Masson Goldner staining. The sections show tissue architecture and cellular details clearly. Special detection of enzyme activity inside bone samples was demonstrated by Tartrate-Resistant Acid Phosphatase (TRAP) staining after laser microtomy, implicating that the laser cutting did not destroy the enzymes. Immunohistochemistry was demonstrated for antigens such as Osteopontin, CD31 or SMA. The results demonstrate that thin sections prepared by laser microtomy can be applied to investigative histopathology applying immunohistochemistry and that antigens are not impaired by laser sectioning. RNA-analysis of 3D-cell clusters cut out of native tissue along an implant interface for biochemical analysis showed that laser cutting does not destroy the biochemical information of the tissue. The opposite is true. Overall RNA-expression was significantly higher (>1000-fold) than from tissue samples prepared by mechanical methods due to the gentle and fast preparation. Clear site-specific TNF-alpha expression at the bone-implant interface could be demonstrated.

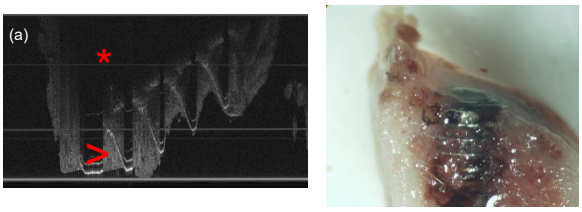

Fig. 1: Image guided tissue preparation at bone-implant interface for RNA analysis.

DISCUSSION & CONCLUSIONS: Femtosecond laser based tissue sectioning does not interfere with enzyme activity, antigen integrity or gene expression of the tissue. It opens a new range of possibilities for histological analysis of hard and implanted tissues and beyond, for site specific biochemical tissue analysis.

REFERENCES: [1] C. Kunert-Keil et al (2019) Histological comparison between laser microtome sections and ground specimens of implant-containing tissues. *Annals of Anatomy* **222**:153–157. [2] C. Gabler et al. (2018) In Vivo Evaluation of Different Collagen Scaffolds in an Achilles Tendon Defect Model. *BioMed Research International* **208.** [3]A. Boyde et al. A distinctive patchy osteomalacia characterises Phospho1 deficient mice. *Journal of Anatomy* **231:**298-308

ACKNOWLEDGEMENTS: We thank Dr. O. Omar (University Gothenburg) for provision of sample and performing molecular biological analysis.

Differential protein adsorption of surface treated Nitinol alloys regulates blood activation

K Gegenschatz-Schmid[1], S Buzzi[2], J Grossmann[3], B Roschitzki[3], D Glück[4], A Zucker[2], M Ehrbar[1]

[1] Laboratory for Cell and Tissue Engineering, Department of Obstetrics, University and University Hospital Zurich, Switzerland. [2] Qvanteq AG, Zurich, Switzerland. [3] Functional Genomics Center Zurich, University of Zurich/ETH Zurich, Switzerland. [4] Blood Transfusion Service SRC Zurich, Switzerland

INTRODUCTION: Stents were developed for overcoming heart attacks and strokes caused by atherosclerosis and their use extended in recent years to the treatment of aneurysms as flow-diverting stents. Due to interaction with foreign material surfaces and blood flow perturbation, a possible complication of stent implantation is thrombosis (blood clot formation). A novel surface treatment developed by Qvanteq AG renders the surface highly hydrophilic and was shown to reduce platelet adhesion and subsequent clot formation on cobalt-chromium surfaces; this effect was shown to be controlled by differential protein adsorption during blood contact (1).

For peripheral and neurovascular stents the typical material is the nickel-titanium alloy Nitinol. In this study we investigated the effect of the surface treatment on this material in terms of blood contact activation and protein adsorption.

METHODS: Nitinol discs and braidings were tested. Discs were electropolished and passivated whereas the wires of the braidings were thermally oxidized after electropolishing.

Sample preparation and surface treatment were performed analogously to what was described in (2). To investigate the tendency to blood coagulation, treated and untreated Nitinol braidings were incubated statically for 1h in fresh, minimally heparinized whole human blood. Assessments consisted of one side in the visual observation of potential clots on the devices and on the other side in the measurement of thrombin-antithrombin complex (TAT) concentration in the blood by ELISA.

For quantification and identification of protein adsorption on untreated and treated Nitinol discs, samples were incubated with minimally heparinized blood plasma. Quantification of adsorbed blood plasma proteins was performed as described (1) using a QuantiPro BCA assay kit. Proteins were digested with trypsin and peptides were desalted using C18 Stage Tips. Desalted peptides were analysed using a state-of-the-art nanoUPLC-MS/MS system at the Functional Genomic Center Zurich. Protein identification and quantification were done with Mascot and ProgenesisQI, respectively. Further functional analysis was performed with PANTHER and KEGG web applications.

RESULTS: Surface-treated Nitinol devices showed a strong reduction in thrombogenicity, indicated both by the absence of large clots in the visual observation and by a significantly lower TAT concentration compared to untreated devices.

Out of 252 identified proteins with a differential abundance between treated and untreated alloys, 120 proteins were identified with a significant p-Value (≤0.05). Three proteins (PROZ, PROC and coagulation factor X) were found with a significant higher abundance on the treated discs, the remaining 117 had a higher abundance on the untreated discs. 34 proteins were annotated to the KEGG pathway "Complement and coagulation cascades", including the 3 proteins with higher abundance on the treated alloys.

DISCUSSION & CONCLUSIONS: Surface treatment of Nitinol alloys reduced blood activation and the total amount of adsorbed proteins. Most of the abundant proteins identified by MS correlated with blood coagulation and activation cascade. Whether the anticoagulants PROC and PROZ, both with higher abundance on treated alloys, or other identified proteins are the major effectors for the anticoagulating effect of the treatment, will be focus of future experiments.

REFERENCES: [1]V. Milleret, S. Buzzi, P. Gehrig, A. Ziogas, J. Grossmann, K. Schilcher, A.S. Zinkernagel, A. Zucker, M. Ehrbar (2015) *Protein adsorption steers blood contact activation on engineered cobalt chromium alloy oxide layers.* Acta Biomater. 24: 343–51. [2]V. Milleret, A. Ziogas, S. Buzzi, R. Heuberger, A. Zucker, M. Ehrbar (2015) *Effect of oxide layer modification of CoCr stent alloys on blood activation and endothelial behavior.* J. Biomed. Mater. Res. B. Appl. Biomater. 103: 629–40.

ACKNOWLEDGEMENTS: R. Urbanet is acknowledged for technical support.

Annulus fibrosus (AF) differentiation of human bone marrow stem cells on biofabricated polycaprolactone scaffolds with oriented multi-lamellar architecture

AJ Vernengo[1,2], Z Li[1], S Grad[1], D Eglin[1], M Alini[1]

[1] AO Research Institute Davos, AO Foundation, Davos, CH. [2] Rowan University, Henry M. Rowan College of Engineering, Glassboro, NJ

INTRODUCTION: The goal of this work is to 3D print multi-lamellar scaffolds with oriented struts composed of polycaprolactone (PCL) mimicking the angle-ply architecture of the annulus fibrosus (AF). In this study, human mesenchymal stem cells (hMSCs) were seeded on the scaffolds, and viability, morphology, and extracellular matrix (ECM) formation were evaluated.

METHODS: Scaffolds were seeded with hMSCs (female, age 55, 540,000 cells per scaffold). Cells were cultured in MSC growth medium for 48 hours to allow for proliferation, at which point the medium was changed to induce AF differentiation using 10 ng/mL TGF-β3 (designated as day 1). At day 28, cell morphology was assessed with AlexaFluor™ 488 Phalloidin counterstained with 4′,6-diamidino-2-phenylindole (DAPI) nuclear stain. Cell viability was evaluated with Live/Dead. Collagen I, II, and aggrecan deposition were evaluated with immunocytochemistry (ICC). DNA and glycosaminoglycans (GAG) assays were performed after 1 and 28 days of culture.

RESULTS: There was a small but significant ($p<0.05$) increase in DNA content of the scaffolds over the culture period. DNA was measured as 3.8 ±0.24 µg at day 1 and 4.6 ±0.43 µg at day 28. GAG, normalized to DNA content (Figure 1), increased over the culture period (20.63 ±5.96 to 278.78 ±22.67) indicating enhanced tissue formation, attributable to the stimulatory effect of the culture medium. Phalloidin stain (Figure 2A) revealed a homogenous cell distribution and attached morphology. High viability was observed with Live/Dead staining (Figure 2B). Collagen I, collagen II, and aggrecan, the major ECM components of the AF, were detected on the scaffold by ICC (Figure 2C-H).

DISCUSSION & CONCLUSIONS: Results indicate the potential of the scaffolds to support regeneration of AF tissue. Gene expression studies are ongoing.

ACKNOWLEDGEMENTS: The authors express thanks to Nora Goudsouzian and Mauro Bluvol for ICC technical support, Robert Peter for support with the biochemical assays, and Christoph Sprecher for assistance with the microscopy.

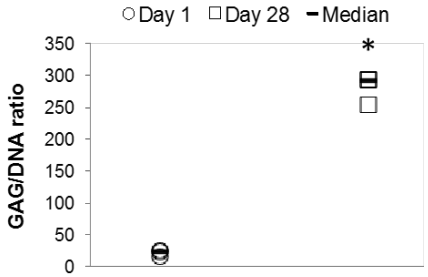

Figure 1. *GAG/DNA ratio for PCL scaffolds after 1 and 28 days of culture. (*) depicts significant differences with respect to day 1 ($p < 0.05$).*

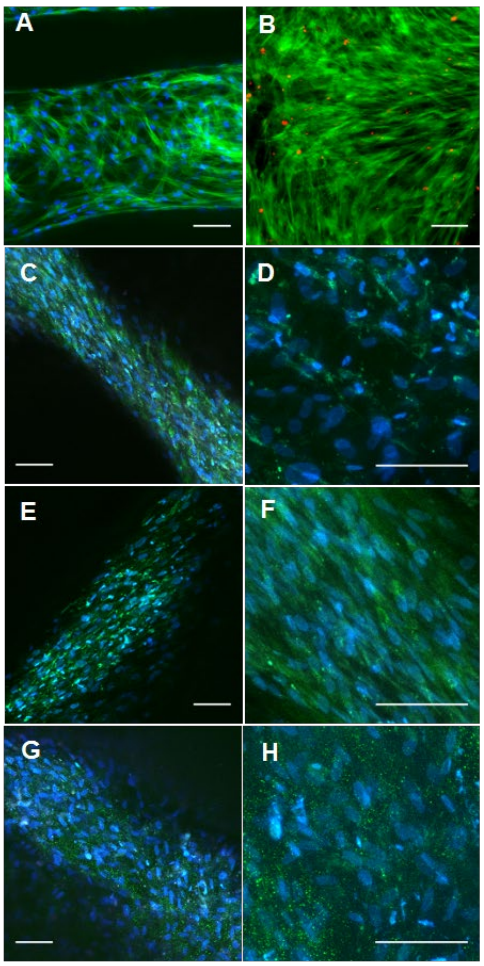

Figure 2. *Fluorescent images of hMSCs on PCL scaffolds at 28 days of culture.* ***(A)*** *F-actin filaments (green),* ***(B)*** *live/dead stain,* ***(C,D)*** *aggrecan,* ***(E,F)*** *collagen I, and* ***(G,H)*** *collagen II (green) immunostaining counterstained with DAPI (blue). Scale bars = 100 µm.*

Blow-spun crosslinked gelatine scaffolds for tissue culture

J Graef[1], J Koeser[1]

[1] *Institute for Chemistry and Bioanalytics, School of Life Sciences, FHNW, Muttenz, CH*

INTRODUCTION: Blow-spinning represents a facile method for the production of fibrous mats. It does not require special equipment and compared to electrospinning has been reported to have 10 times higher deposition rates [1]. Here we evaluate the suitability of this process for the production of highly porous gelatine scaffolds for applications in tissue engineering.

METHODS: Gelatine from either cold water fish (dissolved in water) or gelatine type A (in formic acid) were blow spun employing a custom built coaxial needle with an ID of 0.508 mm. Fiber mats were collected on different supports ranging from aluminum foil to filter paper. Various crosslinking procedures reported in the literature were evaluated with respect to stabilization of the fiber mats upon incubation in aqueous solutions [2]. Rat2 fibroblast cell attachment and survival when cultured on the crosslinked scaffolds was evaluated three days after seeding by dead/live staining and scanning electron microscopy (SEM). Images were focus stacked and assembled applying the Fiji/ImageJ software.

RESULTS: Gelatine based fiber mats were produced by blow-spinning from gelatine solutions. The process was compatible with gelatine solutions in water (typically 60% cold water fish gelatine [3]) or formic acid (typically 20% gelatine type A). The process was stable within a range of different spinning rates ranging from 0.5 ml/hr to 3 ml/hr, and samples of 10 x 25 cm could be easily produced by collecting the spun fibers on different support materials on a rotating drum (Fig 1a). Parallel fiber alignment however was difficult to achieve with on average 32.7% of fibers being within a range of 30° as determined by image analysis using Fiji/ImageJ (Fig 1b). For applications in tissue culture gelatine based scaffolds have to be crosslinked to prevent their dissolution in aqueous environments. For us incorporation of a diglycidyl ether based crosslinker in the spinning solutions and post-spinning crosslinking by heating to 140°C was more efficient than other methods reported in the literature for crosslinking of gelatine based scaffolds like exposure to glutaraldehyde vapour or incubation in ethanolic EDC solutions. Prior to the seeding of cells on the scaffolds they were incubated ON in cell culture medium to release/inactivate potentially cytotoxic unreacted crosslinker. Such treated blow-spun gelatine scaffolds had a thickness of 1-2 mm when incubated in aqueous solutions, were not cytotoxic as proven by dead/live staining (Fig 1d) and rat2 fibroblasts were found frequently to spread between fibers rather than attaching on only single fibers (Fig 1c).

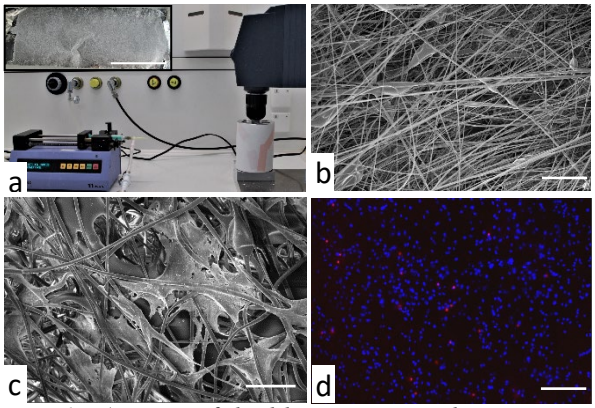

Fig. 1: a) setup of the blow-spinning device, inset: blow spun sample on aluminum foil support; SEM images of blow spun gelatine scaffolds prior to incubation in aqueous solutions (b) and following cell colonization (c); d) dead(red)/live(blue) staining of rat2 cell nuclei growing on a cross-linked gelatine scaffold. Scalebars: a) 10 cm, b) 100 µm, c) 20 µm, d) 200 µm.

DISCUSSION & CONCLUSIONS: Here we present data on the evaluation of the blow spinning process for the production of gelatine based fiber mats as scaffolds for tissue culture. The process does not require elaborate equipment and produces samples with suitable sizes for tissue culture applications. While within the presented project we demonstrated the stability of the scaffolds in aqueous solutions and their cytocompatibility, in the future we plan to evaluate their suitability for 3D perfusion culture.

REFERENCES: [1]J.L. Daristotle, A.M. Behrens, A.D. Sandler et al (2016) *ACS Appl Mater Interfaces* **8(51)**: 34951–34963. [2]N. Reddy, R. Reddy, Q. Jiang (2015) *Trends Biotechnol.* **33(6)**:362-9. [3]F. Liu, R.J. Avena-Bustillos, C. Bilbao-Sainz et al (2017) *J Food Sci*. **82(6)**:1402-1411.